UNIVERSITY OF MINNESOTA
ST. ANTHONY FALLS HYDRAULIC LABORATORY

Project Report No. 141

The Use of Standard Bodies to Measure the Cavitation Strength of Water

by
EDWARD SILBERMAN,
FRANK R. SCHIEBE,
and
EDWARD MROSLA

This research was sponsored by the Office of Naval Research, U.S. Navy, under Contract N00014-67-A-0113-0032.

SEPTEMBER 1973
MINNEAPOLIS, MINNESOTA

CONTENTS

LIST OF ILLUSTRATIONS

LIST OF TABLES

ABSTRACT

Research has been conducted to evaluate a technique for measuring the cavitation strength of water. The technique is based on counting cavitation events as a function of cavitation number on a standard body, thereby producing cavitation characteristic curves. It is assumed that water cavitates because of nuclei carried in the water and that the measured characteristic curves must therefore be related to the nuclei which are present.

In this research it was hypothesized that the nuclei, whatever their real nature, could be represented by a distribution of equivalent gas bubbles of neutral density. The standard bodies were designed according to potential flow theory so that the bubble trajectories, along with their cavitation rates, could be calculated. By calculating cavitation characteristic curves for various bubble numbers and size distributions and comparing the calculated curves with measured curves for the same body, it was possible to infer the specifications for the equivalent bubble nuclei that were present in any test. The equivalent nuclei can be described using N, the number of cavitatable bubbles per unit volume of water (a number far smaller than the total number of nuclei per unit volume); r_{max}, the likely radius of the largest bubbles in the distribution; and a, a parameter of the exponential size distribution assumed for the bubbles.

As a consequence, given (N, r_{max}, a) and an experimental realization whose flow field can be calculated by potential flow theory, it should be possible to predict incipient cavitation. The experiment devised for verifying this statement proved to be faulty, and experimental verification has not yet been accomplished.

An alternative for future study has been proposed which calls for abandoning the hypothesis of equivalent bubble nuclei and determining the relative cavitation strength of water by direct comparison of a measured cavitation characteristic curve obtained on a standard body in a specific test configuration with a catalogue of such curves kept on file for a family of standard bodies.

The present research is, in a sense, an extension of earlier work supported by the Naval Ship Systems Command, General Hydromechanics Research program under Contract N00014-67-A-0113-0020.

THE USE OF STANDARD BODIES TO MEASURE THE CAVITATION STRENGTH OF WATER

I. INTRODUCTION

The inability to predict cavitation inception and to reproduce inception measurements in scale models is one of the unsolved problems in hydromechanics. The problem was well illustrated by the scattering of results of measurements of inception obtained when the ITTC headform was tested in water tunnels throughout the world [1]*. Yet it is desirable that a method be found to reduce the results of measurements in different experimental realizations to a common basis. This report describes some research directed toward the problem of designing and developing a "standard cavitator" for this purpose.

Some of the background of the problem is outlined in the next chapter. It is observed that the principal reason for the discrepancies in inception measurements is the variation in cavitation nuclei in the streams of the various facilities in which the tests are conducted. Consequently, the problem has been approached from the viewpoint of developing a mechanism to characterize the nuclei occurring in any given test stream.

A method previously developed for calculating cavitation occurrence rates on standard, theoretically designed bodies [2] was adapted to this purpose. The calculation method is reviewed and updated in Chapter III. It involves the following elements: (1) Representing the nuclei by a suitable equivalent gas bubble distribution; (2) designing a family of standard bodies with progressively variable minimum pressure coefficients whose flow and pressure fields can be readily predicted; (3) preparing a program which calculates the number of cavitation events associated with the passage of any given equivalent gas bubble distribution past any given body of the family as a function of cavitation number; (4) measuring in a test facility the number of cavitation events near inception as a function of cavitation number for flow past a body of the family (the resulting curve is called a "cavitation characteristic"); and (5) comparing the measured cavitation characteristic with calculated characteristics for several assumed gas bubble distributions to infer the nucleus distribution in the test stream.

---

*Numbers in brackets refer to list of references on pages 27 and 28.

If this method were completely successful, the nuclei characteristics of two test streams could be compared as to their cavitation potentialities; indeed, one stream might be made, by trial and error, to have similar characteristics to another for test purposes by adjusting air content, filtering, and other water treatments. Thus the cavitation inception point of an arbitrary body in a natural environment could be predicted by testing it in a water tunnel whose water characteristics had been adjusted to be equivalent to those of the natural water.

In Chapter IV, some new experimental work which was designed to test the analytical model is described. This did not prove very useful for the purpose due to experimental difficulties with cavitation occurrence counting resulting from cavitation in the jet boundaries of the test stream. Nevertheless, the insight gained from these experiments, as well as from some earlier experiments also described in this chapter, was instrumental in developing the bubble distribution function used in the analytical model.

Chapter V summarizes the findings of this research and outlines the proposed method of procedure. It also contains suggestions for an alternate system in which the attempt to characterize nuclei in a test stream would be completely abandoned, but the standard body and cavitation counting concepts of the present scheme would be retained. It was not possible to carry out research on the feasibility of this alternate system in the present program.

Cavitation number is defined herein by

$$\sigma = \frac{p_o - p_v}{\frac{1}{2} \rho U_o^2} \tag{1A}$$

and pressure coefficient by

$$-c_p = \frac{p_o - p}{\frac{1}{2} \rho U_o^2} \tag{1B}$$

where p_o, U_o, and ρ are the pressure, velocity, and density in the uniform flow ahead of a test body; p_v is the vapor pressure of the test water; and p is the pressure at a point on the test body or in the fluid.

II. THE PROBLEM OF THE STANDARD CAVITATOR

Although the attempt to compare cavitation inception measurements using the ITTC headform was frustrating from the viewpoint of obtaining comparable measurements, it did lead to a great deal of discussion regarding the reasons for the discrepancies. The principal reasons can be grouped under five headings. These will be discussed in the first five sections following, after which the course pursued in the present research will be outlined.

A. Problems with the ITTC Headform Tests

1. Cavitation Nuclei. Probably the major cause for discrepancy in experimental results lies in the variation in nuclei contained in the water of the various test facilities [3,4]. Although it is possible that variations in body surface material also contribute to the problem [5], the scattering in results obtained from the tests on the ITTC headform point to the nuclei in the water as the more important source.

The real problem concerns description of the nuclei--what are they and what are their size distributions? Minute gas bubbles with or without particulate inclusions and stable hydrophobic particles with gas trapped in their crevices are likely nuclei in water tunnels and towing tanks [6,7]. In natural water bodies, minute organisms might be added to these [2]. The nuclei are probably of microscopic size, say 1 to 100 microns in diameter. Some speculations about nuclei are contained in Appendix I.

It is generally agreed that gas is trapped in nuclei. The local water pressure must approach the gas pressure before cavitation can occur. Because of surface tension, hydrophobic particles may begin to cavitate when the trapped gas is at a slightly higher pressure than the local vapor pressure, but for spherical bubbles, cavitation can begin only when the local pressure surrounding a nucleus decreases below vapor pressure. For a spherical bubble this critical pressure can readily be calculated [8, for example] and becomes increasingly less than vapor pressure as the bubble size decreases. Calculation is not possible for hydrophobic particles. Nuclei cavitate when they are carried by the stream past the low pressure (or "superheated") region of a submerged body provided the pressure on the body or in the eddies produced by the flow is sufficiently low. A true vapor cavity is characterized by the fact that it will collapse suddenly when it leaves the superheated region. (Pseudocavitation produced by the expansion of larger gas

bubbles in accordance with the gas laws when bubbles pass through a low pressure region is excluded from this discussion. Such bubbles do not collapse suddenly.)

The problem of comparing the ITTC headform measurements would have been considerably simplified if the characteristics of the nuclei in each test facility could have been evaluated. Whereas the nuclei in specific natural water bodies, and even in towing tanks, can be considered relatively stable with time and with varying operating conditions, the situation is entirely different in water tunnels. The operation of the tunnel pump, its air removal facilities, the pressure at which a given experiment is run, the original source of water, and other factors all contribute to the nuclei population. Hence, the nuclei vary from one experiment to the next in a given tunnel as well as from tunnel to tunnel. An example of the mixture of nuclei that occurs in a specific tunnel is described by Peterson [6].

Perhaps the most direct way of describing the nuclei would be to photograph them using holographic techniques as Peterson has done [6]. But this is very tedious, since many holograms must be obtained and analyzed in order to amass sufficient data for satisfactory statistical accuracy. It was thought at one time that acoustic resonance phenomena might be used to measure gas nuclei sizes, but this proved to be impractical because of inability to distinguish adequately between the small bubble size ranges that occur [9]. Other techniques have been tried--for example, optical counting and sizing by measuring light scattering as single bubbles pass through a very small control volume while illuminated by a laser beam [10] and counting and sizing particles electrically as they pass through an orifice [11]. One of the limitations on most methods is that if they are to be useful in water tunnel testing, they must be capable of operating at test section conditions [12]. Methods which depend on withdrawing samples may be adequate for natural waters or towing tanks, but they are generally not so for water tunnels, where most such testing is done.

The present research, which will be described later, was directed principally at overcoming this problem of nucleus identification.

2. Identifying Cavitation Inception. In accordance with the original instructions, those making measurements on the ITTC headform used their customary methods for determining when cavitation occurred. These methods varied considerably, most of them being dependent on visual observation,

and this probably contributed toward the discrepancies in results. One of the problems is that the number of cavitation events necessary to assure detection, whatever the method used, depends on body size. This problem is discussed in Chapter III, section C. The introduction of cavitation occurrence counting by Schiebe [13] and its development and adoption by others [14] have gone far toward improving methods of identifying cavitation inception. This method counts the number of cavity collapses occurring near the body by sensing the resulting pressure pulses. Results are reproducible, but there is a limitation if separation occurs near the test body and produces cavitation before the normal body cavitation occurs. The problem is discussed in section 5 below. An optical counting method developed by Keller [10] would overcome this limitation, but there would be physical problems in its use in large-scale experiments, especially since it would only count occurrences in the vicinity of one predetermined point on the body.

3. Effects of External Boundaries. This problem is well brought out by Hoyt's discussion of the original presentation of data on the ITTC headform tests [15]. A body will have a different pressure distribution within constrained boundaries than in unconfined flow; hence, incipient cavitation may be different. It is possible to carry out potential flow calculations for velocity and pressure distribution on bodies without and with external boundaries using computers [16], and this should be done preceding experiments to assure that the model flow is not excessively constrained.

4. Nuclei Screening. Assuming that nuclei vary both in kind and in size distribution from one test realization to another, nuclei will follow various trajectories past a given body and possibly experience different superheats at a given cavitation number. Johnson and Eisenberg [17] outlined the problem relative to spherical gas bubbles and Peterson [6] calculated some typical trajectories and corresponding changes in bubble size for comparison with his experiments. The basic method of bubble trajectory calculation is presented by Johnson and Hsieh [8], and a computer program for the purpose developed at the Naval Ship Research and Development Center was used by Peterson. Trajectory calculations, along with knowledge of the pressure field about the body and of the initial pressures for specific

bubble sizes, permit calculation of the cavitation potential for a given bubble passing through the flow field if its upstream position is known.

The calculation methods are for pure gas nuclei. As previously noted, it has been argued by many that the important nuclei may not be gas bubbles. Schiebe has postulated that for bodies large compared to the nuclei, the nuclei closely follow the streamlines on the average [2] and trajectory variation is not an important consideration, after all. A supporting argument can be found in Appendix I.

5. Boundary Layer Separation. If the boundary layer separates, the low-pressure point in a given test may occur in a separation eddy rather than in the potential flow field about the body. Arakeri [18] has shown both analytically and experimentally that laminar boundary layer separation did occur on the ITTC headform tested in two facilities at the California Institute of Technology. In his calculation, Arakeri used Thwaites's method for calculating the momentum thickness of two-dimensional boundary layers as modified for axially symmetric flow [19, pp. 430-432] together with two-dimensional criteria for separation [19, p. 306]. His calculation was based on the potential pressure distribution on the headform. A similar calculation conducted for the present investigation and reported in Appendix II also predicts laminar separation on this body. Although more sophisticated methods for calculating boundary layer separation are available (step-by-step calculation, for example [20]), the method used by Arakeri is known to work on blunt bodies, and his experimental verification (using a Schlieren technique) seems to confirm the occurrence.

Somewhat less blunt bodies than the ITTC headform apparently should be used as standard cavitators to avoid the possibility of laminar boundary layer separation. Of course, tunnel boundary conditions can influence separation as well as cavitation inception by altering the pressure field. A body which does not experience separation in infinite fluid may do so under tunnel constraint conditions. However, transition to turbulence may prevent laminar separation and its attendant low pressure regions if speeds are sufficiently great.

There is a secondary problem associated with separation. Even if separation does not occur in the immediate vicinity of the low pressure point of the body, where cavitation is usually expected, it may occur at

the rear of the body or on the tunnel boundaries. Using an acoustic method of counting bubble collapses, the collapses from bubbles produced in these separated areas are as readily counted as those occurring in the low pressure region. This problem arose in tests conducted for the present research program in an open jet test section wherein it was discovered that early cavitation was occurring in the shear layer of the jet and was being counted by the detection device as though it were occurring on the test body. Further discussion of this matter is contained in Chapter IV, section B, part 2.

B. The Present Program

The present research program was undertaken as a step toward developing a standard cavitator while avoiding as many of the pitfalls discussed above as possible. It is possible to design a family of standard body shapes which will be free from separation on the nose near the low pressure point and to make the body diameter small enough in any given facility that the surrounding pressure field will be essentially that for infinite fluid. As has already been noted, occurrence counting as presently used should eliminate most human errors in detecting cavitation inception. If the nuclei are gas bubbles, their trajectories can be calculated, but for the present purpose they are simply assumed to follow the streamlines; in any event, the cavitation susceptibility of various nuclei can be calculated. This leaves as the remaining uncontrolled variable the nuclei themselves.

It is the purpose of this research to infer information about the nuclei in a given test facility by comparing the cavitation characteristic of a standard body during test operations with calculated characteristics for that body based on various nucleus distribution assumptions. To this end, several gas bubble distribution patterns were tested analytically to assess their usefulness in reproducing cavitation characteristics obtained by measurement. Further, the distribution obtained by this means using measurements on one of the standard bodies was to be verified by predicting and measuring the cavitation characteristic of another of the standard bodies in the same water, although the cavitation inception point would differ somewhat between the two bodies. The analytical work is described in Chapter III and the experimental work in Chapter IV.

III. AN ANALYTICAL MODEL

The analytical model for the standard cavitator is based on the work of Ref. [2], which is summarized and extended herein.

A. Assumptions

The fundamental assumptions are

1. For the cavitation nuclei (see Appendix I):
   a. Nuclei occur and are stabilized in the entraining water by a variety of mechanisms. A nucleus, however stabilized, has for cavitation stability purposes an equivalent gas bubble size.
   b. The cavitation inception point for an individual nucleus is determined by the isothermal, static stability criteria of its equivalent gas bubble.
   c. Nuclei have the same average density as water.
   d. Nuclei are randomly distributed in the test water in a homogeneous manner.
   e. There is no diffusion of gas through a nucleus wall.
   f. There is no interaction in the flow field among nuclei.
2. For the standard body:
   a. The flow field is axisymmetric.
   b. The body can be designed for any desired pressure distribution using potential flow theory and can be made separation-free in the low pressure region using boundary layer calculations.
   c. The body diameter is very large compared to the nuclei and the resulting cavitation bubbles and very small compared to the external flow boundaries.

B. The Standard Body

The standard bodies are selected from a series generated by placing uniform disk sources in a uniform stream. Van Tuyl [21] suggested such

bodies for cavitation studies. The computations in Ref. [2] are based on the work of Sadowsky and Sternberg [22]. The bodies are identified by their minimum pressure coefficients, $C_{p,min}$. Body surface coordinates and surface pressures are given in Appendix I of Ref. [2] for 15 such bodies varying from $C_{p,min} = -0.333$ (point source) to $C_{p,min} = -1.000$, and some typical streamlines and pressure distributions in the fluid are also given. Laminar boundary layer calculations for these bodies are summarized in Appendix II and show that all bodies are separation-free. Three of these standard bodies were selected for further analysis: $C_{p,min} = -0.333$, $C_{p,min} = -0.45$, and $C_{p,min} = -0.60$. For these bodies the shapes of the streamtubes have been calculated, as have the pressure distributions in the flow field.

C. Cavitation Occurrence Calculation

1. The Calculation Process. With the flow field specified by selection of a standard body, the number of cavitation events occurring on the body can be predicted if the number of equivalent gas bubble nuclei and their size distributions are known and the operating cavitation number is specified. The calculation begins with subdividing the flow field into a number of streamtubes, j, beginning with one whose boundary is the standard body. The pressure along each stream surface is calculated, and from this the average $C_{p,min}$ within each streamtube is estimated. With the cavitation number set equal to $-C_{p,min}$ at the outer edge of the first streamtube adjacent to the body, the critical radius of a bubble which will just cavitate is calculated. This is converted to pressure (and temperature) conditions in the uniform flow upstream of the body using the gas laws and including surface tension effects for subsequent comparison with the size distribution of the approaching nuclei. All bubbles in the approaching distribution which are larger than critical will cavitate, and all smaller will not, at this specific cavitation number.

The process is repeated j times with the cavitation number each time set equal to $-C_{p,min}$ at the edge of a streamtube successively farther from the body. For each repetition, the critical bubble radius is calculated for each streamtube; the critical radius in the streamtube adjacent to the body will become larger as the cavitation number is increased, and fewer bubbles in that tube will cavitate; similarly for the succeeding tubes.

The bubble size distribution is specified in histogram fashion by dividing the complete range of radii into i subranges, all of equal radius increment. Then, for each of the j streamtubes at each repetition a weighting coefficient can be established to indicate whether a given bubble subrange will cavitate under the specified operating conditions. If the bubble radius subrange is larger than critical, the weighting coefficient will be unity; if smaller it will be zero; and if it straddles critical, the coefficient will lie between zero and unity, its value depending on the critical radius compared to the subrange limits. For each of the j repetitions, the weighting coefficients for each subrange from all the streamtubes are added together to produce a coefficient c_{ij}. Here i refers to the bubble subrange and j to the specific repetition; $0 \leqslant c_{ij} \leqslant i_{max}$. The matrix c_{ij} is determined once the standard body and its operating σ are specified. The entire calculation can be summarized by

$$n_j = c_{ij}\, m_i \tag{2}$$

where m_i is a column matrix representing the bubble radius distribution and n_j is a row matrix representing the number of cavitation events at each repetition. To facilitate the calculation, $j_{max} \equiv i_{max}$, making c_{ij} a square coefficient matrix; this means the number of streamtubes must equal the number of size subranges in the bubble distribution.

In the present work, Eq. (2) has been normalized by writing m_i for the fraction of the bubble population occurring in each radius subrange. The matrix c_{ij} must then also include a specification for the radius increment at each i. To obtain the actual cavitation occurrence rate at each repetition, both sides of Eq. (2) must be multiplied by the number of bubbles per unit time being transported through each streamtube. In the calculation, the outer limit of the outer streamtube is selected so that very few of the nuclei will cavitate beyond this distance from the body under operating conditions. (All streamtubes beyond that are immaterial to the calculation.) The boundaries of all the streamtubes are drawn to produce equal discharges in all tubes; this means there are equal streamtube areas in the uniform flow approaching the body. Since the equivalent bubble nuclei were assumed to be randomly and homogeneously distributed, equal numbers of nuclei with similar size distributions are transported through each streamtube. If the nucleus population is N per unit volume, the transport is Nq per streamtube where q is the

flow rate per streamtube. The cavitation occurrence rate at each cavitation number can now be written

$$M(\sigma) = \sum_{j=1}^{j_{max}} Nq[n_j] = Nq \sum_{j=1}^{j_{max}} [c_{ij}(\sigma,R)][m_i] \qquad (3)$$

where R specifies the radius increment for each i. A computer program in Appendix II of Ref. [2] solves this equation given m_i and i_{max}, N, $C_{p,min}$ of the standard body, σ, R, the velocity of flow, and the streamtube area. The program assumes that a decrease in σ will be obtained through a decrease in pressure. The program could be readily rewritten to use a constant pressure with decreases in σ produced by increases in velocity.

If bodies of different sizes and the same shape are to be compared, it is desirable to divide both sides of Eq. (3) by a reference area. This could be the body cross-sectional area or a streamtube area. The left side of Eq. (3) will then yield an occurrence rate per unit area, and on the right side q will be replaced by a velocity; this is the uniform, free stream velocity if the reference area is the streamtube area--as it is in the program of Ref. [2]. (When comparisons are being made between experimental realizations, it is especially desirable to record counts per unit area where the area is specified. The discrepancies in identifying cavitation inception discussed in Chapter II, section A, part 2 may well be attributable to subconscious rejection of cavitation events below a certain minimum.)

Schiebe and Killen found it desirable to specify the radius distribution in 16 subranges in order to represent well the true, continuous bubble size spectrum in some of their work [9]. In subsequent work, $i_{max} \equiv j_{max} \equiv 16$ has been used. This produces a 256 element matrix c_{ij}; however, with σ close to $-C_{p,min}$, most of the elements are zero, and even for smaller σ many are zero. The selected radius distribution is taken to exist in the uniform flow upstream of the test body at a standard pressure (and temperature) corresponding to the reference cavitation number and reference velocity chosen for water tunnel tests. In towing tank or open water work, the radius distribution corresponds to the pressure (and temperature) at mean body depth.

2. Bubble Distribution Assumptions. It has been the hypothesis of this chapter that there exists an equivalent gas bubble size distribution m_i which characterizes the test water in any cavitation experiment and that if that size distribution is known, along with the concentration of bubbles, N, the number of cavitation events can be calculated using Eq. (3). In some preliminary work, Schiebe calculated a few occurrence rates for the $C_{p,min} = -0.333$ body and compared them with measured rates [23]. He used 16 subranges of 1×10^{-5} ft radius increment. The plotted comparison indicated reasonable results, but to get these results Schiebe had to guess N as well as a suitable bubble radius histogram. The 16 parameters required to specify the histogram made it very inconvenient to make many trials to match calculated and measured occurrence rates. Also, it was not determined whether his data set (N,m_i) was unique for that operating condition.

An attempt was made early in the present program to determine m_i by solving the linear Eq. (3) using a calculated matrix c_{ij} and measured cavitation occurrence rates M for a standard body. Several problems made solution impractical. A major one occurred because the solution requires inversion of c_{ij}. But when numerical values were substituted in the calculation, it turned out that the determinant of the matrix was nearly zero. (If the determinant had been truly zero, it would have implied that a unique solution did not exist.) Contributing to this, the matrix c_{ij} is only as realistic as the assumptions outlined earlier permit it to be. Since the true matrix is unknown, the error involved in obtaining m_i would also be unknown; this problem is discussed by Segel [24]. A further problem is that when $M(\sigma)$ is measured in an experiment, it turns out to be a stochastic function and cannot be given with great precision.

To pursue the matter further, it was decided to continue using the trial-and-error process, but to facilitate computation by reducing the number of parameters. This can be done by using a continuous curve to represent the histogram type of distribution for m_i even though the generality of the bubble distribution spectrum is thereby constrained. Two measured cavitation characteristic curves were selected from the data obtained for Ref. [23] for making the trials. These are displayed in Figs. 1 and 2, the former being for the ITTC headform and the latter for the $C_{p,min} = -0.333$ halfbody. The method used to obtain these data is outlined in Chapter IV, section B.

At first, a logarithmic-normal distribution with two parameters, mean radius $\bar{r}$ and its standard deviation v, was used to establish m_i. The log-normal distribution appeared to be a reasonable one to represent real bubble size distributions. Computations were made for 16 subranges of 1×10^{-5} ft radius increment. Good comparisons were obtained with the measured data in Figs. 1 and 2, as can be seen in Figs. 3 and 4. But it can also be seen from the data in these figures that the results are not unique; widely different combinations of m_i and N can reproduce the measured curve equally well.

As a consequence of this discovery, it was thought that a separate method of determining N would make it possible to infer a unique distribution m_i. Some exploratory work in direct measurement of N and reference to work done by Hammitt and his coworkers in this area [25, for example] dispelled this idea. The problem is that although there are a great many bubble nuclei in a given water sample, only a small part of the spectrum (the larger bubbles) is involved in cavitation inception and in the solution of Eq. (3). Actually, $\bar{r}$ in the log-normal model was below the cavitating range in all trials because of the large number of small bubbles. Even if the log-normal distribution were a very good representation of the true bubble spectrum, a scheme based on measurements of cavitation inception could not provide information about the parameters of that distribution.

It is now apparent that what is required for m_i is a characterization which is valid for the larger cavitatable bubbles of the distribution regardless of how poorly that characterization may fit the smaller bubbles. Several distributions are possible, and some have been tried. These include a quadratic distribution, the Cauchy distribution, an exponential distribution, and even a uniform distribution ($m_i = 1/16$ for all i). Hopefully, with a suitable distribution, a unique set (N, m_i) could be obtained by trial and error to match by calculation any arbitrary measured cavitation characteristic. The number of bubbles per unit volume, N, would then be the number above some minimum cavitatable size.

Of the distributions tried, the exponential distribution in the form

$$m_i = \frac{e^{-a\frac{i-1}{i_{max}}} - e^{-a\frac{i}{i_{max}}}}{1 - e^{-a}} \qquad (4)$$

was the best and has been selected for further use. Here a is the only parameter of the distribution if i_{max} is assigned ($i_{max} = 16$ in the present work); $a = 0$ gives the uniform distribution $m_i = 1/i_{max}$, while $a \gg 1$ gives $m_i = 0$ for large i.

The measured cavitation characteristics could be reproduced well by Eq. (4), and at first it seemed that there existed a unique set (N,a) to describe the equivalent gas bubbles. This notion was questioned when it was realized that another parameter had been incorporated into the solutions of Eq. (3) by using 16 radius increments of 1×10^{-5} ft each. Introducing a larger (or smaller) maximum radius by changing the number of increments or the size of each causes the uniqueness problem to arise again. However, the calculated range in numbers of cavitatable bubbles was very much less for the exponential distribution with reasonable ranges of the parameters than it was for the log normal distribution. Typical calculated data points are shown in Figs. 5 and 6, together with values for N and a, in comparison with the measured data of Figs. 1 and 2. The method of calculating data points is outlined in Appendix III. It appears from these figures that the number of cavitatable bubbles, N, is almost uniquely determined by this calculation, although there is still some uncertainty introduced by varying r_{max} and a.

It can be seen in Figs. 5 and 6 that to reproduce a measured characteristic, the parameter a has to increase as the maximum radius increases; the number of cavitatable bubbles also generally increases, but only slightly. An increase in a to accommodate an increase in r_{max} means that there are proportionally fewer of the added larger bubbles than there were of the previous largest size; a decrease in a means that there are proportionally more of the new largest sized bubbles than there were of the largest size range that was removed. These tendencies counterbalance the trends toward change in bubble numbers and account for the reduced range in predicted numbers of cavitatable bubbles using the exponential distribution.

These results were considered sufficiently satisfactory that the exponential distribution has been adopted for further calculations. The equivalent bubble nuclei are given by a set (N,a,r_{max}) in which N can be determined almost uniquely for any experimental realization by the proposed model, but a and r_{max} appear to be indeterminate. It must be observed, however, that for any assumed r_{max} there is a unique value of a, and vice versa.

These parameters together measure the shape of the characteristic curve, and a compatible pair (a, r_{max}) must accompany each N in order to specify the equivalent gas bubble nuclei. If it is realized that r_{max}, like M, is a stochastic variable with a considerable range for successive trials in any given experiment, the indeterminateness of the pair (a, r_{max}) is both reasonable and acceptable in the model.

3. The Number of Streamtubes. The use of 16 streamtubes in all calculations is quite arbitrary and came about almost accidentally because of the earlier work by Schiebe and Killen [9]. Peterson has suggested that nuclei must actually reach the body surface to cavitate [6], which would mean that under the present assumptions only the first streamtube was important. The computer program presented in [2] makes it possible to take $i_{max} \neq 16$. An attempt was made to match the data in Figs. 1 and 2 using $i_{max} = 1$ by the method just described. It was not possible to produce satisfactory data points with this single streamtube by the calculation methods proposed herein. Whether there is some other number smaller than 16 which could be used has not been investigated.

D. Use of the Model

There are three kinds of uses to which the analytical model might be put in combination with measured cavitation characteristic curves. These are

1. Predicting incipient cavitation for a specific test of a body whose stream surfaces and pressure distribution are calculable. The nuclei in the water in the test facility would first be characterized by measuring a cavitation characteristic using a standard body in the facility at a σ near the expected incipient point. A set (N, a, r_{max}) so determined would be used in subsequent calculations. This is the method proposed for validating the analytical model and will be discussed in Chapter IV.

2. To compare the nucleus characteristics of waters in two test realizations in which tests have been made of the same or different models of a given body or of the body itself. The sets (N, a, r_{max}) would again be determined from measured characteristics on standard bodies in each of the realizations. The standard bodies would be mounted adjacent to (if the separation

could be made sufficiently great) or in place of the body being tested. Hopefully, variations in nuclei characteristics would at least explain the differences in test results, if differences occurred, and might be useful in correlating the measurements.

3. To investigate the effect of changing water characteristics, such as aerating or deaerating, on the nuclei properties. Figure 7, which uses some of the earlier data collected by Schiebe on the ITTC and $C_{p,min} = -0.333$ bodies [23], illustrates what might be done. The figure indicates, for example, that an increase in total air generally increases the number of cavitatable bubbles, other conditions being held constant.

The real utility of the analytical model will depend upon its validation by appropriate experiments and by experience gained with its use.

IV. VALIDATING THE MODEL

A. Proposal for Validation

The following steps can be used to test the hypothesis on which the concept of the standard cavitator and its analytical model are based:

1. Design a standard body to operate at a predetermined $C_{p,min}$ in a water tunnel or other facility.
2. Test the standard body in that facility to obtain cavitation rate M versus cavitation number σ over a range in σ while all other variables are held as constant as possible. This will produce a cavitation characteristic curve.
3. Try various sets of assumptions for a and r_{max} in Eqs. (3) and (4) for the equivalent gas bubble nuclei until the shape of the cavitation characteristic is reproduced. Then find N, the number of cavitatable nuclei. The method is outlined in Appendix III.
4. Calculate the cavitation characteristic for another body using the set (N,a,r_{max}) just determined and test this second body in the same facility with the same water as soon after the first test as possible. For water tunnel testing, the $C_{p,min}$ of the second

body must not vary too far from that of the first in order to avoid changing nuclei by large changes in tunnel speed or pressure.

Correct prediction of the cavitation characteristic for several different pairs of bodies would be considered validation of the method. Failure to predict could be due to one of the problems outlined in Chapter II or to inappropriateness of the method.

B. Experimental Work

An experimental program was devised to test the concept of the standard cavitator according to the preceding steps. It was designed to be carried out in the open-jet test section of the six-inch water tunnel at the St. Anthony Falls Hydraulic Laboratory. The open-jet section was chosen to permit the use of larger test bodies than could be used with the closed-jet section used in the work of Ref. [23]. The planned program, described in section 2 following, was unsuccessful, however, and a substitute program was established based on data obtained previously for use in Ref. [23]. This work is described in section 3.

1. The Six-Inch Water Tunnel. This facility is a more or less conventional form of recirculating water tunnel with provision for employing either 6 in. dia. closed-jet or open-jet test sections. The area contraction is 30:1 from a 30 in. sq. settling section to the 6.18 in. dia. test section. It is powered for about 50 fps maximum velocity in the test section and can operate at pressures down to the vapor pressure of water.

This tunnel is different from other conventional tunnels in that it contains a gas separator unit installed in the square settling section just upstream of the contraction. The gas separator unit is a tunnel reach filled with a packet of small flow tubes, each with a crown shaped to a sharp, inverted V in which a greatly thickened boundary layer develops. The larger entrained gas bubbles passing through these tubes manage to gravitate upward into this boundary layer within the length of the tube and are there exposed to a relatively low velocity and a weakened transporting system. The tube axis is tilted downward in the direction of flow so that the bubbles collecting in the crown of the tube will be subject to a gravitational force component acting upstream along the top of the tube.

Standard galvanized, corrugated steel sheets were stacked to produce tube lengths of 3 ft at an angle of about 20 degrees with the horizontal in the device. For the fixed tube slope, collection and upstream movement of bubbles greater than some critical size occurs depending on the velocity through the tubes--that is, the velocity in the test section. This acts as a filter with a gradual cutoff characteristic with size. It is analogous to an electric filter in this respect. The separation process is enhanced by coalescence of the bubbles in the crown of each tube, increasing bubble size and velocity. The individual tubes are provided with holes near the upstream end which permit the bubbles to gravitate from one tube to the next above. The bubbles progress upward through the tube stack to the top of the tunnel conduit, where they are collected and bled off to a vacuum control tank.

The operating procedure for the tunnel is the same as that used previously [23] for the closed-jet test section. Total gas content in the tunnel water is measured using a conventional van Slyke apparatus. Water samples for this purpose are tested immediately before and after a test run using a bypass tube from just upstream to just downstream of the test section. It is customary to make test runs using fresh water each day. The total gas content is regulated by deaerating the tunnel water, which is accomplished by operating the tunnel with heavy cavitation and draining off the collected gas through the gas separator. After deaeration to 4 to 5 ppm, the tunnel water can be reaerated to any desired level by opening a stop cock in the test section while the tunnel is operating. Cavitation number is usually controlled by setting a constant tunnel speed and decreasing pressure in small increments.

2. Open-Jet Test Section Experiments. The open-jet test section housing is 15 inches in diameter by 13 inches long from the end of the nozzle to the beginning of the receiving cone connecting with the diffuser. Two velocity profiles taken across the open-jet test section 2.25 in. downstream from the nozzle are shown in Fig. 8.

Test bodies were designed using disk sources in a uniform stream as described in Chapter III, section B. Bodies with $C_{p,min} = -0.333$ (point source), -0.45, and -0.60 were constructed. These were of 2 in. ultimate diameter with a 3 in. long nose section and a 7 in. long tail section. The

bodies were designed to be installed in pairs as shown in Fig. 9. This permits the changing of bodies without disturbing the tunnel water simply by sliding the support mechanism across the test section. It facilitates carrying out step 4 of the validation. Only the nose sections were designed for the given shapes. The tail sections and support structure were contained in a single unit which remained permanently in the test section while noses were changed.

Eight noses were constructed as shown in Table 1. The noses were all machined to design shape using photographs taken at twice full size for guidance. Final verification of the construction and effect of tunnel constraint was obtained from experimental pressure measurements. These are shown in Table 2. All the measurements were made at about 15 fps test section velocity to avoid cavitation.

Table 1 -- STANDARD DISK SOURCE BODIES

$C_{p,min}$	-0.6	-0.45	-0.33
Lucite with pressure taps	X	X	X
Delrin with internal transducer	X	X	X
Teflon with internal transducer	X	none	X

The bodies with internal transducers were used for cavitation counting. The transducer was a Clevite ceramic cylinder model PZT-5. It was mounted on the end of a metal tube such that the position of the transducer was about one inch from the nose of the body. The cavity in which the transducer was placed was filled with castor oil to allow the transmission of pressure signals from the body wall to the transducer. Coaxial cable was led out from the body through the support system. The transducer signal was amplified and converted into a square voltage pulse by a single shot multivibrator. This was necessary so that the initial pulse and subsequent transducer ringing due to resonance and bubble rebounding and recollapsing would be converted into a single, clean step signal. Both the amplified transducer signal and the square pulse were monitored on an oscilloscope to assure a proper

Table 2 -- PRESSURE DISTRIBUTION ON TEST BODIES

a. $C_{p,min} = -0.333$

Axial Dist. from Nose, In.	C_p Calc.	C_p Meas.
0.000	+1.00	+1.00
0.100	+0.543	+0.559
0.250	+0.094	+0.044
0.500	-0.250	-0.221
0.650	-0.318	-0.242
0.800	-0.333	-0.364
0.950	-0.320	-0.297
1.200	-0.274	-0.285
1.800	-0.165	-0.182
2.600	-0.087	-0.091

b. $C_{p,min} = -0.45$

Axial Dist.	C_p Calc.	C_p Meas.
0.000	+1.000	+1.000
0.060	+0.648	+0.585
0.416	-0.450	-0.427
0.596	-0.412	-0.415
0.796	-0.346	-0.336
1.096	-0.259	-0.245*
1.696	-0.148	-0.167
2.496	-0.079	-0.090

*Average of two readings

c. $C_{p,min} = -0.600$

Axial Dist.	C_p Calc.	C_p Meas.
0.000	+1.000	+0.985
0.036	+0.717	+0.644
0.220	-0.600	-0.579
0.680	-0.359	-0.375
0.980	-0.260	-0.260
1.580	-0.147	-0.173
1.980	-0.105	-0.136

triggering level of the multivibrator. The effect of changing trigger level sensitivity on counts of cavitation events is shown by the data in Fig. 2. It is very important that a consistent level be used. The pulses were counted on a commercial electronic counter. Figure 10 is a schematic diagram of the arrangement.

Delrin and Teflon were chosen as body surface materials to permit eventual comparison of these hydrophilic and hydrophobic materials in the

tunnel. The tests would be useful in determining the relative importance of stream nuclei as opposed to surface nuclei under the various operating conditions of this tunnel. The plastic, Delrin, is known to have approximately the same acoustic impedance as water (though slightly larger), so that there is little loss in transmission of pressure pulses occurring in water through the Delrin body and oil filling. Teflon body material also has impedance characteristics similar to those of water (slightly smaller). Hence it is not expected that comparative tests will be influenced by acoustic impedance.

It became apparent soon after the cavitation test runs were begun that the number of measured cavitation events was excessive. High occurrence rates were being measured on all bodies at cavitation numbers well above $-C_{p,min}$, even at low air contents. Figure 11 shows a typical result. The tests were repeated using some 5/8 in. dia. bodies available from earlier tests in the closed-jet tunnel with the same unexpected results. Air leakage into the test section through the body mounts and vibration of the bodies were suspected at first, but these possible causes were eliminated. Exploration by several other devices finally made it appear probable that the collapse counts were of cavities generated in the shear layer between the jet and the "dead water" region surrounding it rather than cavities generated on the body. The cavities are collapsing somewhere downstream of the transducer location and near the outer radius of the jet, but they are still being counted by the detector. A longer nozzle projecting into the open jet housing would probably be required to eliminate this cavitation.

It was believed at first that changing the trigger level setting might eliminate the spurious counts, but there is so little attenuation of these sonic pulses in water that this is not useful. Another technique tried was bucking two transducers in a pair of test bodies located as shown in Fig. 9 against each other. Collapses near the edge of the jet between the two bodies would then be nearly equidistant from the transducers and would tend to cancel each other, while those close to one body would not be canceled out. There was some reduction in count with this method, but for the method to be fully effective, the outside transducer would have to form a complete ring around the jet without generating cavitation itself. Designing such a transducer did not seem practicable at this stage of the research.

It was finally decided to abandon these tests for the present and examine what might be done with data previously obtained in the closed-jet test section where there was little, if any, separation.

3. Analysis of Closed-Jet Test Section Data. During previous experiments on cavitation counting, one of the authors collected much cavitation characteristic data on the ITTC headform and the $C_{p,min} = -0.333$ halfbody in the closed-jet test section [23]. Typical data for the halfbody are reproduced in Fig. 12. Some of these data have already been used in Chapter III, sections C and D. The bodies tested had ultimate diameters of 5/8 in. and were made of Delrin. They contained transducers and electronic circuitry similar to that described for the open-jet test section. To check on the possibility that the ITTC headform cavitation might have been affected by separation, a calculation for laminar separation was made and is summarized in Appendix II. This confirmed that such separation was possible. At the same time, however, the Reynolds number at the separation point is of the order of 3×10^5 or higher for all the data used. It is believed that transition to turbulence prevented separation for those tests.

Since the pressure fields were known theoretically for both bodies, the first criterion for testing a standard body had been met. The pressure fields and streamlines are given in Ref. [23]. The second testing requirement, obtaining the measured cavitation characteristics, was met by data already in hand from the experiments. The third requirement is to match the measured characteristics with calculated characteristics using assumed equivalent bubble size distributions and numbers of bubbles. The method for doing this is outlined in Appendix III, and some results have been discussed in Chapter III.

The matching is not quite as straightforward as it may appear, because each data point in Figs. 1 and 2 represents an average for M of about ten measurements at each σ. The occurrence rate is a stochastic phenomenon, and a large number of repetitions of measurements is necessary to establish a relationship. As it is, there is no smooth curve defining $M(\sigma)$, but such a curve has been drawn by eye in the figures and been used for matching purposes. It is now apparent that the parameter a in the exponential distribution is a measure of the shape of a mean characteristic curve. Repetitions of the measurements could be expected to lead to different values of a for each repetition. These variations no doubt represent real stochastic

variations in the nuclei approaching the body. Since only the available data have been used for analysis, it has not been possible to measure the probable variation in a (or in N and r_{max}) for many repetitions. It is believed, however, from the results presented in Chapter III, that N, the number of cavitatable bubbles per unit volume, would be little influenced by variations in a to match small changes in the shape of the $m(\sigma)$ curve.

The fourth step in the validation process cannot be carried out with the data in hand. The two bodies tested are too far apart in $C_{p,min}$ (-0.60 and -0.333) to permit using the nuclei characteristics measured with one to predict the characteristic curve of the other. The disparity is illustrated by the results portrayed in Fig. 7. Thus, although the available data from the closed-jet test section contributed greatly to establishing the analytical model, they are not adequate to validate it.

C. Validity of the Model

An unfortunate selection of test facility has negated attempts to verify the analytical model experimentally. By the time the problem with the open-jet test section was discovered, so much of the contract funds and time had been expended that it was not feasible to undertake a new experimental investigation as part of the present program.

Nevertheless, by using available data from earlier experiments in a closed-jet test section, an apparently self-consistent analytical model has been developed for describing equivalent gas bubble nuclei in a test facility. The model permits good analytical reproduction of measured cavitation characteristic curves as shown in Figs. 5 and 6 and predicts some of the expected trends in incipient cavitation with changes in air content as shown in Fig. 7. The reproduction of measured characteristics is, by itself, no assurance that the model is valid, as was demonstrated by the earlier false starts using a log-normal bubble distribution. But the fact that each measured characteristic, using the finally chosen exponential distribution in the analytical model, has associated with it an almost unique number of cavitatable bubbles per unit volume does give considerable credence to the model. This, together with the results portrayed in Fig. 7, suggests that the model may be valid.

It is still necessary to conduct an experimental validation, and one should be planned and carried out. In the meantime it is believed

that this model can be used to explain divergent results in incipient cavitation measurements in various facilities.

V. SUMMARY -- PROSPECTS FOR A STANDARD CAVITATOR

It has been pointed out that the principal reason for discrepancy among test realizations in predicting cavitation inception is the variability in cavitation nuclei in the water. All the other possibilities for discrepancy can and should be controlled in cavitation testing so that their influence is made minor.

It has been proposed that the variability in nuclei be measured by a device called a standard cavitator. This device would, in effect, measure the cavitation strength of the water in the experiment. This report has examined a model for such a device. It consists of a series of standard bodies designed by potential flow theory for a range of $C_{p,min}$ values. The bodies contain acoustic transducers for counting the cavitation collapses that occur in the water near the body. The curve of collapse rate or cavitation events versus cavitation number then determines a cavitation characteristic for the given body in the given experiment as illustrated in Figs. 1 and 2. The problem is to relate characteristic curves from one experimental realization to those of another realization whose characteristic curves are not identical with the first and, thus, to measure the relative strengths of the waters in the two experiments.

Schiebe proposed that the comparison be made by calculating the rate of cavitation event occurrence for each experiment. The calculated rate would be made identical with the measured rate for that experiment by adjusting certain parameters in the calculation; these parameters measure the number and characteristics of the nuclei. The standard body, having been selected in advance for the experiment, has its pressure and velocity field already fixed and known.

One of the principal assumptions of the model is that the real nuclei, whatever they may be, can be represented by equivalent gas bubble distributions. In this report the distribution of these bubbles is taken to be exponential, because only the largest bubbles contribute to incipient cavitation. Three controllable parameters are available: N, the density per unit volume of cavitatable bubbles in the approaching flow; r_{max}, the bubble

radius likely not to be exceeded; and a, the measure of the shape of the distribution. That measured cavitation characteristics can be represented very well by calculated characteristics when (N, r_{max}, a) are properly chosen is illustrated by Figs. 5 and 6 for two different bodies in a six-inch closed-jet water tunnel, while Fig. 7 shows that the trends in these parameters are in accord with some expectations.

A failure in experimental technique made it impossible to completely validate the model experimentally within the framework of this program. This task remains to be undertaken. Nevertheless, it is believed that the model presents a useful device for comparing the results of incipient cavitation tests in various facilities using the same and different models.

The procedure for nucleus characterization using this model is as follows:

1. Select a standard body whose $C_{p,min}$ is near the expected cavitation number of the experiments to be conducted. This can be done from Appendix I of Ref. [2].

2. Provide the body with an internal transducer and associated electronic circuitry for acoustic occurrence counting as described in Chapter IV, section B. Obtain cavitation characteristics similar to those in Figs. 1 and 2 in the test facility using this body.

3. Set up the computer program for calculating cavitation events on the selected body as in Appendix II of Ref. [2]. Using this computer program and the exponential bubble distribution given by Eq. (4), match a calculated cavitation characteristic curve with the measured one. The matching can be carried out in accordance with Appendix III of this report.

4. As a result of the matching, a set of parameters (N, r_{max}, a) will be obtained. These will characterize the test water under the specific test conditions. It is believed that this set will be unique for this test, although this has not been completely demonstrated.

The most important remaining task in developing this model for the standard cavitator is to devise an experiment in which the equivalent gas

bubble parameters predicted from measurements on a standard body can be used to predict incipient cavitation on another body under the same test conditions. Other tasks include investigation of the stochastic nature of the parameters N, a, and r_{max} and appropriate use of this in the calculations.

There is an alternate plan for a standard cavitator. In this, the attempt to characterize the nuclei or equivalent nuclei would be abandoned, but the standard bodies and acoustic counting to develop cavitation characteristics would be retained. Certainly, two experimental realizations producing identical cavitation characteristic curves for the same standard test body could be said to use waters with equal cavitation strengths. Perhaps a catalogue could be established divided into sections with each section devoted to a single standard body. Within each section there would be standard cavitation characteristic curves for that body obtained from one or more test facilities by varying air content, speed, and other factors. These curves would be identified by numbers. Then a facility making a cavitation test would insert one of the standard bodies, measure its characteristic curve, compare this with the curves for that body in the catalogue, and in its test report identify the cavitation strength of the water by specifying the standard body and curve number from the catalogue. This plan warrants further investigation.

Finally, investigators should be warned about the various pitfalls they may encounter if inadequate attention is given to the factors other than nuclei variability which can lead to discrepancies in incipient cavitation measurement. These were discussed in Chapter II, section A. One such factor that caused a problem in this investigation was the occurrence of cavitation in the shear layer at the edge of an open jet being used as a test facility. The collapsing cavities were counted by the acoustic transducer just as though they had occurred near the body. Similar spurious counts could be obtained from a separation region near the trailing edge of the body if the pressures in the separated eddies were less than those at the low pressure point on the body.

REFERENCES

[1] Lindgren, H. and Johnsson, C. A., "Cavitation Inception on Head Forms, ITTC Comparative Experiments," Appendix V, Report of the Cavitation Committee, Proceedings, 11th ITTC, Tokyo, Japan, 1966, pp. 219-232.

[2] Schiebe, F. R., The Measurement of the Cavitation Susceptibility of Water Using Standard Bodies, Project Report No. 118, St. Anthony Falls Hydraulic Laboratory, 1972.

[3] Hammitt, F. G., "Effects of Gas Content Upon Cavitation Inception, Performance, and Damage," annex to Vol. VI, 64 pp., Proceedings, Fourteenth Congress of the International Association for Hydraulic Research, Paris, France, 1971.

[4] Eisenberg, P., "Environmental and Body Conditions Governing the Inception and Development of Natural and Ventilated Cavities," Appendix I, Report of the Cavitation Committee, Proceedings of the 12th ITTC, Rome, Italy, 1969, pp. 346-350.

[5] van der Meulen, J. H. J., "Cavitation on Hemispherical Nosed Teflon Bodies," IUTAM Symposium on Non-Steady Flow of Water at High Speeds, Leningrad, USSR, 1971, pp. 333-341.

[6] Peterson, F. B., "Hydrodynamic Cavitation and Some Considerations of the Influence of Free-Gas Content," Ninth Symposium on Naval Hydrodynamics, Paris, 1972, 53 pp.

[7] Holl, J. W., "Nuclei and Cavitation," Journal of Basic Engineering, ASME, December 1970, pp. 681-688.

[8] Johnson, V. E., Jr. and Hsieh, T., "The Influence of Trajectories of Gas Nuclei on Cavitation Inception," Sixth Symposium on Naval Hydrodynamics, 1966, U.S. Government Printing Office, pp. 163-182.

[9] Schiebe, F. R. and Killen, J. M., An Evaluation of Acoustic Techniques for Measuring Gas Bubble Size Distributions in Cavitation Research, Project Report No. 120, St. Anthony Falls Hydraulic Laboratory, 1971.

[10] Keller, A., "The Influence of the Cavitation Nucleus Spectrum Inception, Investigated with a Scattered Light Counting Method," Journal of Basic Engineering, ASME, December 1972, pp. 917-925.

[11] Ahmed, O. and Hammitt, F. G., "Determination of Particle Population Spectra from Water Tunnel Using Coulter Counter," Proceedings, 1969 Cavitation Forum, ASME, pp. 26-28.

[12] Morgan, W. B., "Air Content and Nuclei Measurement," Appendix I, Report of the Cavitation Committee, Proceedings of the 13th ITTC, Berlin-Hamburg, Germany, 1972.

[13] Schiebe, F. R., "Cavitation Occurrence Counting - A New Technique in Inception Research," 1966 Cavitation Forum, ASME, New York, pp. 8-9.

[14] Brockett, T., "Cavitation Occurrence Counting - Comparison of Photographic and Recorded Data," 1969 Cavitation Forum, ASME, New York, pp. 22-23.

[15] Hoyt, J. W., "Wall Effect on ITTC Standard Head Shape Pressure Coefficients," Proceedings, 11th ITTC, Tokyo, Japan, 1966, pp. 257-259.

[16] Hess, J. H. and Smith, A. M. O., Calculation of Non-Lifting Potential Flow about Arbitrary Three-Dimensional Bodies, Report No. ES 40622, Douglas Aircraft Division, Long Beach, Calif., 1962, 177 p.

[17] Johnson, V. E., Jr. and Eisenberg, P., "Environmental and Body Conditions Governing the Inception and Development of Natural and Ventilated Cavities," Appendix I, Report of the Cavitation Committee, Proceedings, 11th ITTC, Tokyo, Japan, 1966, pp. 171-181.

[18] Arakeri, V. H., Viscous Effects in Inception and Development of Cavitation on Axi-Symmetric Bodies, Report No. Eng. 183-1, California Institute of Technology, Pasadena, Calif., January 1973, 157 p.

[19] Rosenhead, L., Ed., Laminar Boundary Layers, Clarendon Press, Oxford, England, 1963.

[20] Schlichting, H., Boundary Layer Theory, McGraw-Hill, New York, 1968, pp. 178-180.

[21] van Tuyl, A., "On the Axially Symmetric Flow Around a New Family of Half-Bodies," Quarterly of Applied Mathematics, Vol. 7, 1950.

[22] Sadowsky, M. A. and Sternberg, E., "Elliptic Integral Representation of Axially Symmetric Flows," Quarterly of Applied Mathematics, Vol. 8, 1950.

[23] Schiebe, F. R., The Influence of Gas Nuclei Size Distribution on Transient Cavitation near Inception, Project Report No. 107, St. Anthony Falls Hydraulic Laboratory, 1969.

[24] Segel, L. A., "Simplification and Scaling," SIAM Review 14, 1972, pp. 547-571.

[25] Ahmed, O. and Hammitt, F. G., Cavitation Nuclei Size Distribution in High-Speed Water Tunnel under Cavitating and Non-Cavitating Conditions, College of Engineering, Univ. of Michigan, April 1972, 58 p.

[26] Harvey, E. N.; McElroy, W. D.; and Whiteley, A. H., "On Cavity Formation in Water," Journal of Applied Physics, Vol. 18, February 1947.

[27] Turner, W. R., Acoustic Microbubble Spectrum Analyzer, Continuing Evolution, Vitro Labs, Tech. Note 02242.01-1, Section 3.2, July 1970.

[28] Silberman, E., Air Bubble Resorption, Technical Paper No. 1-B, St. Anthony Falls Hydraulic Laboratory, August 1949, p. 32.

[29] Lieberman, L., "Air Bubbles in Water," Journal of Applied Physics, 28, 1957, pp. 205-211.

ILLUSTRATIONS

(Figures 1 thru 12)

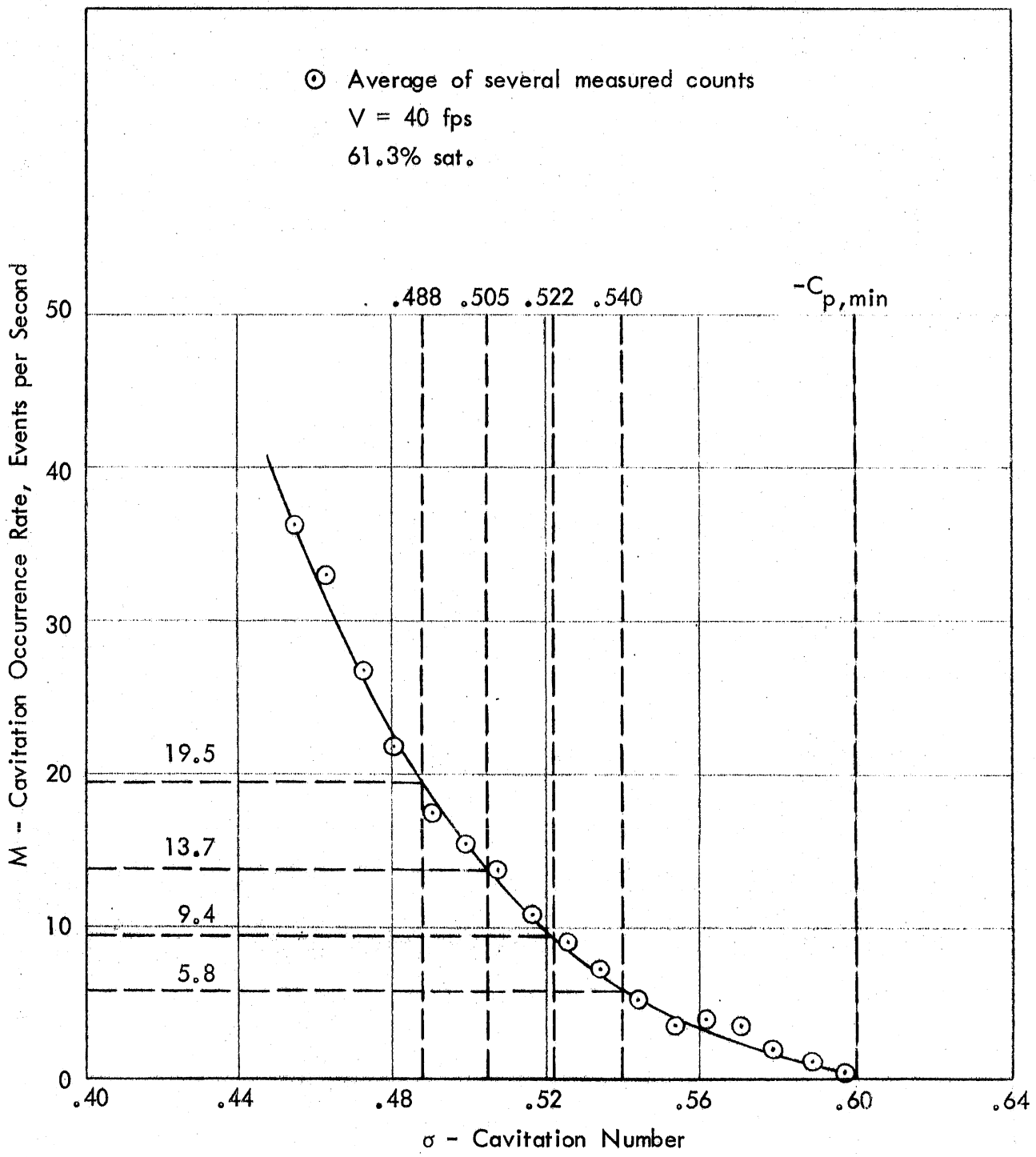

Fig. 1 - Measured Cavitation Characteristic in the Closed Jet Test Section, ITTC Headform [23]

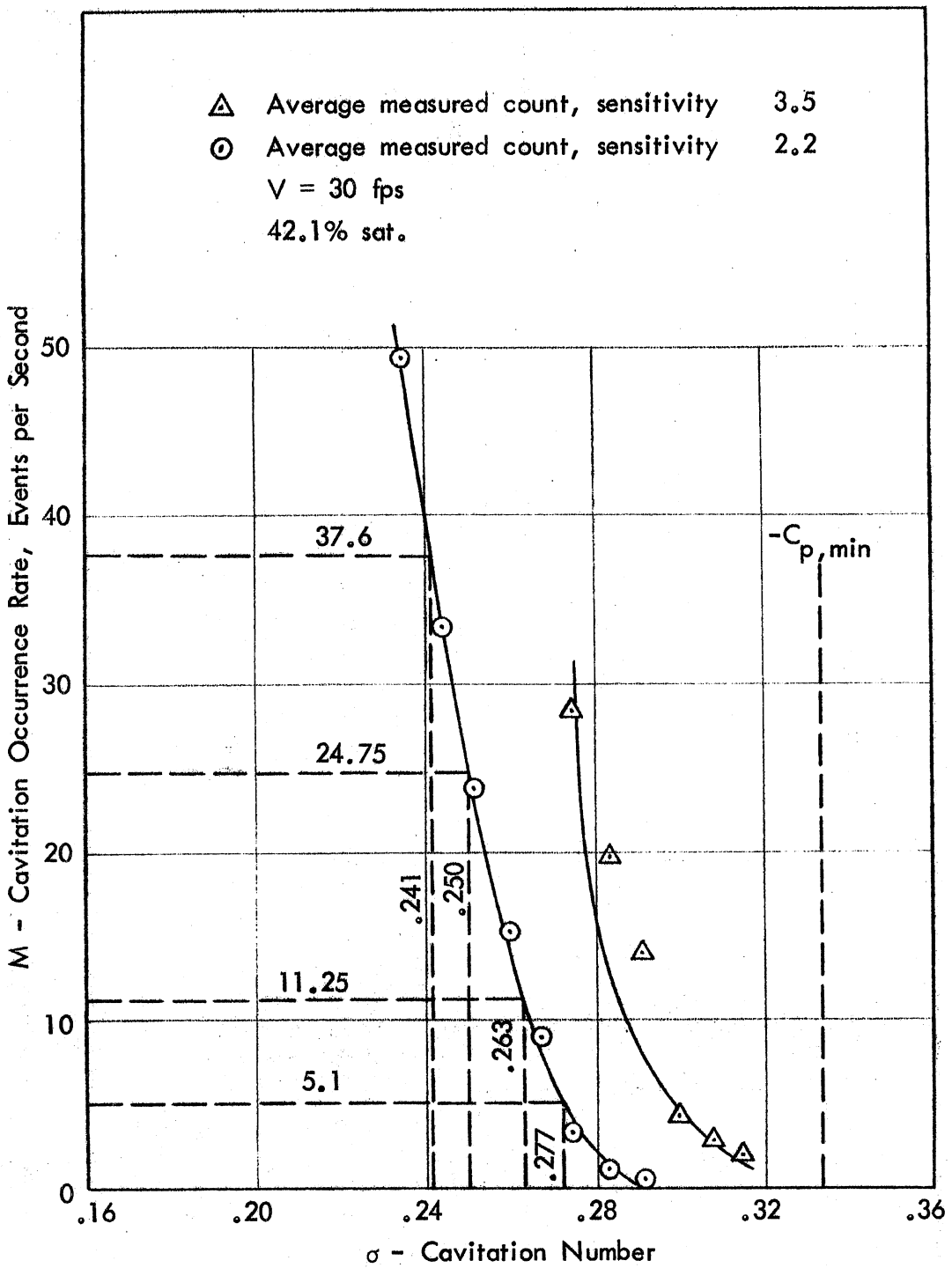

Fig. 2 - Measured Cavitation Characteristic in the Closed Jet Test Section, $C_{p,min} = -0.33$ Body [23]

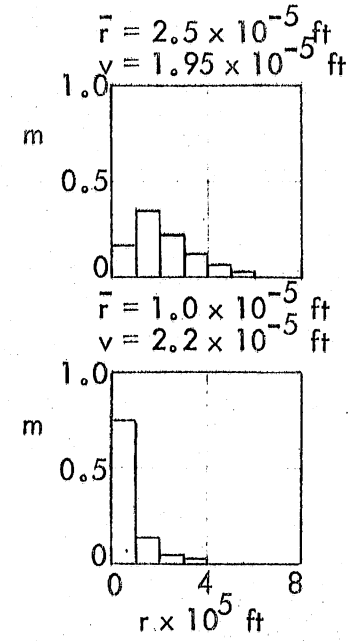

⊙ Average measured collapse rate [23]

△ Calculated

$\bar{r} = 2.5 \times 10^{-5}$ ft

$v = 1.94 \times 10^{-5}$ ft

$N = 4250$ bub/ft^3

⊡ Calculated

$\bar{r} = 1.0 \times 10^{-5}$ ft

$v = 2.2 \times 10^{-5}$ ft

$N = 16980$ bub/ft^3

V = 40 fps
61.3% sat.

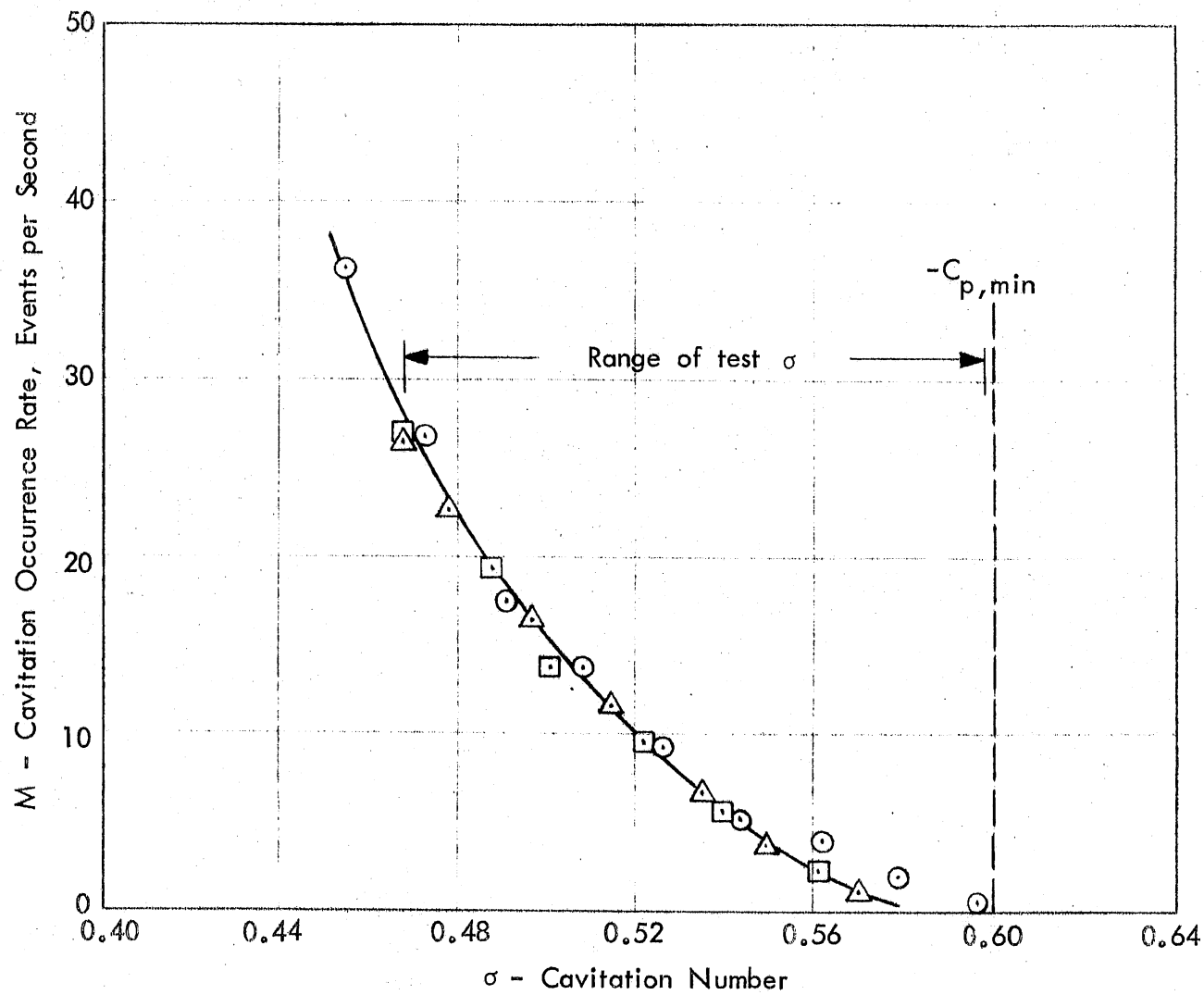

Fig. 3 - Comparison of Calculated Cavitation Characteristic using Log-Normal Distribution with Measured Characteristic, ITTC Headform

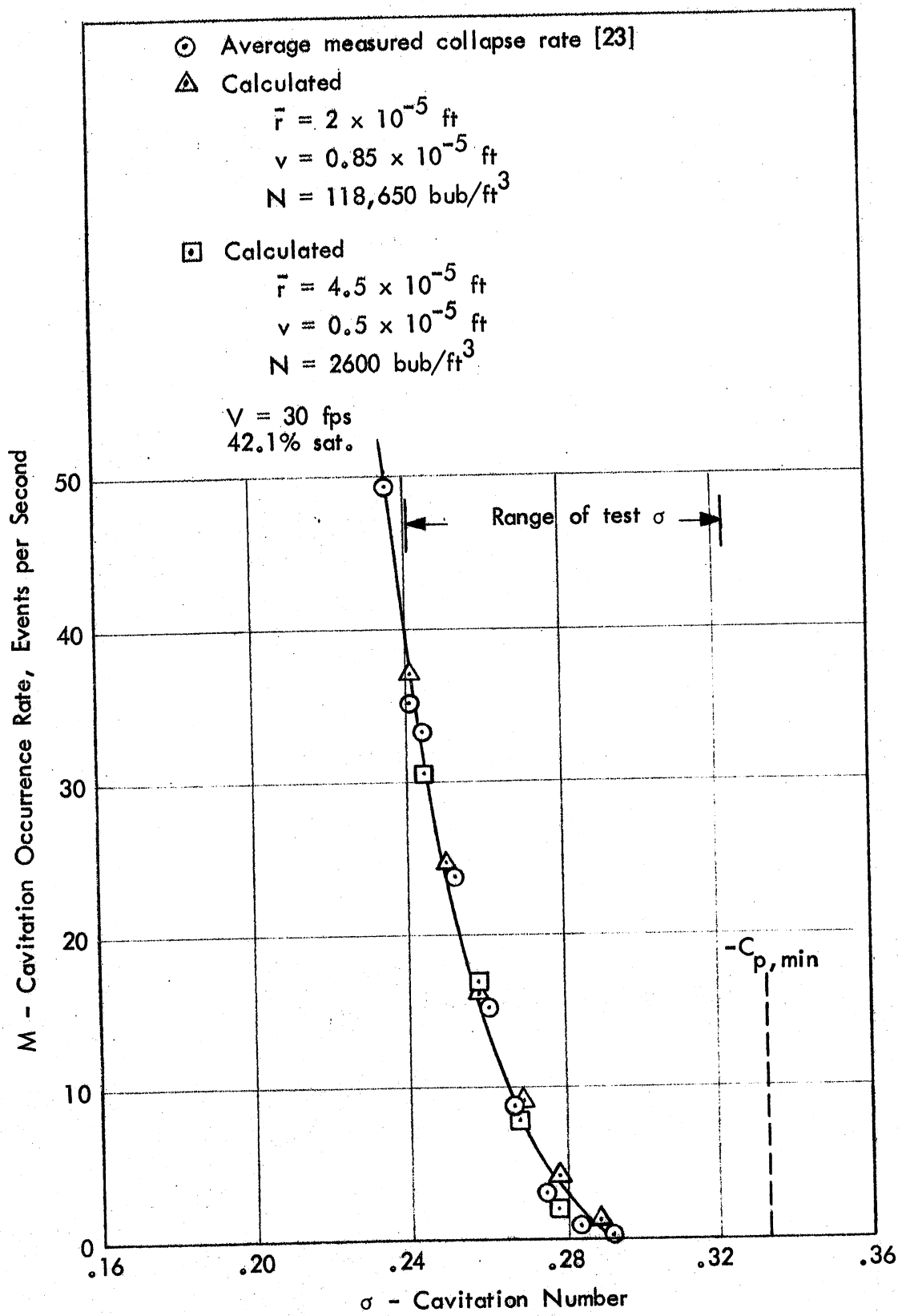

Fig. 4 - Comparison of Calculated Cavitation Characteristic using Log-Normal Distribution with Measured Characteristic, $C_{p,min}$ = -0.333 Body

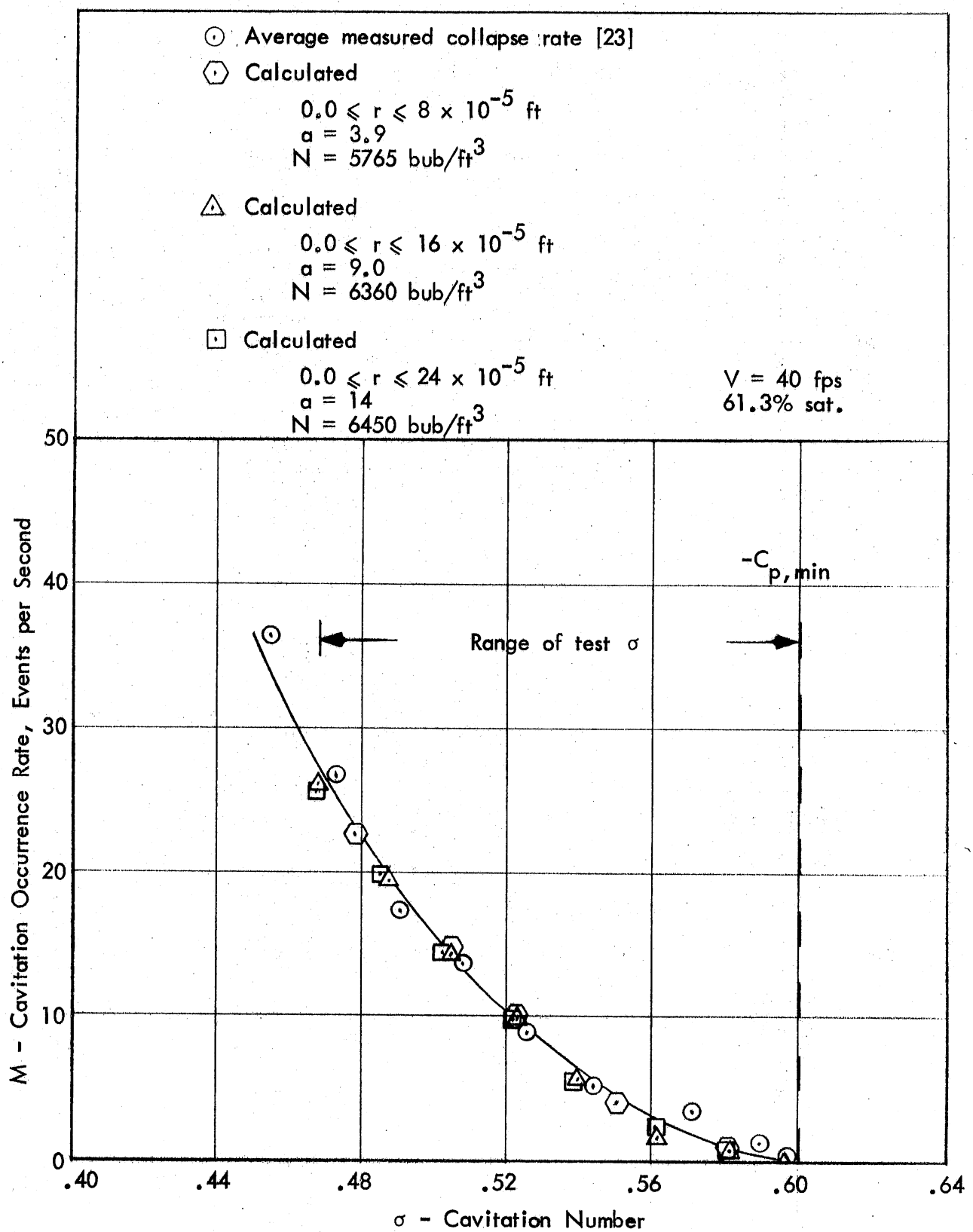

Fig. 5 - Comparison of Calculated Cavitation Characteristic using Exponential Distribution with Measured Characteristic, ITTC Headform

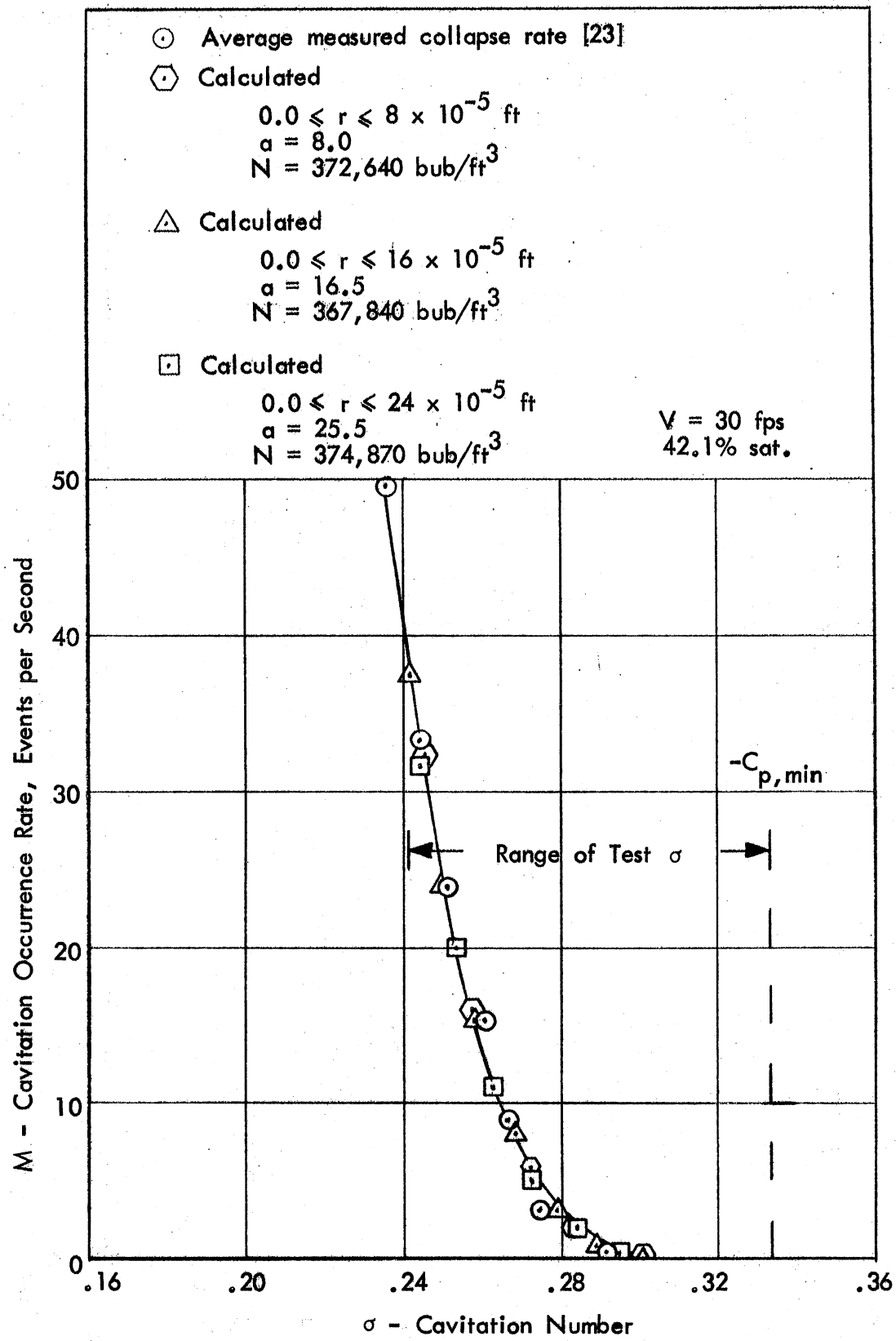

Fig. 6 - Comparison of Calculated Cavitation Characteristic using Exponential Distribution with Measured Characteristic, $C_{p,min}$ = -0.333 Body

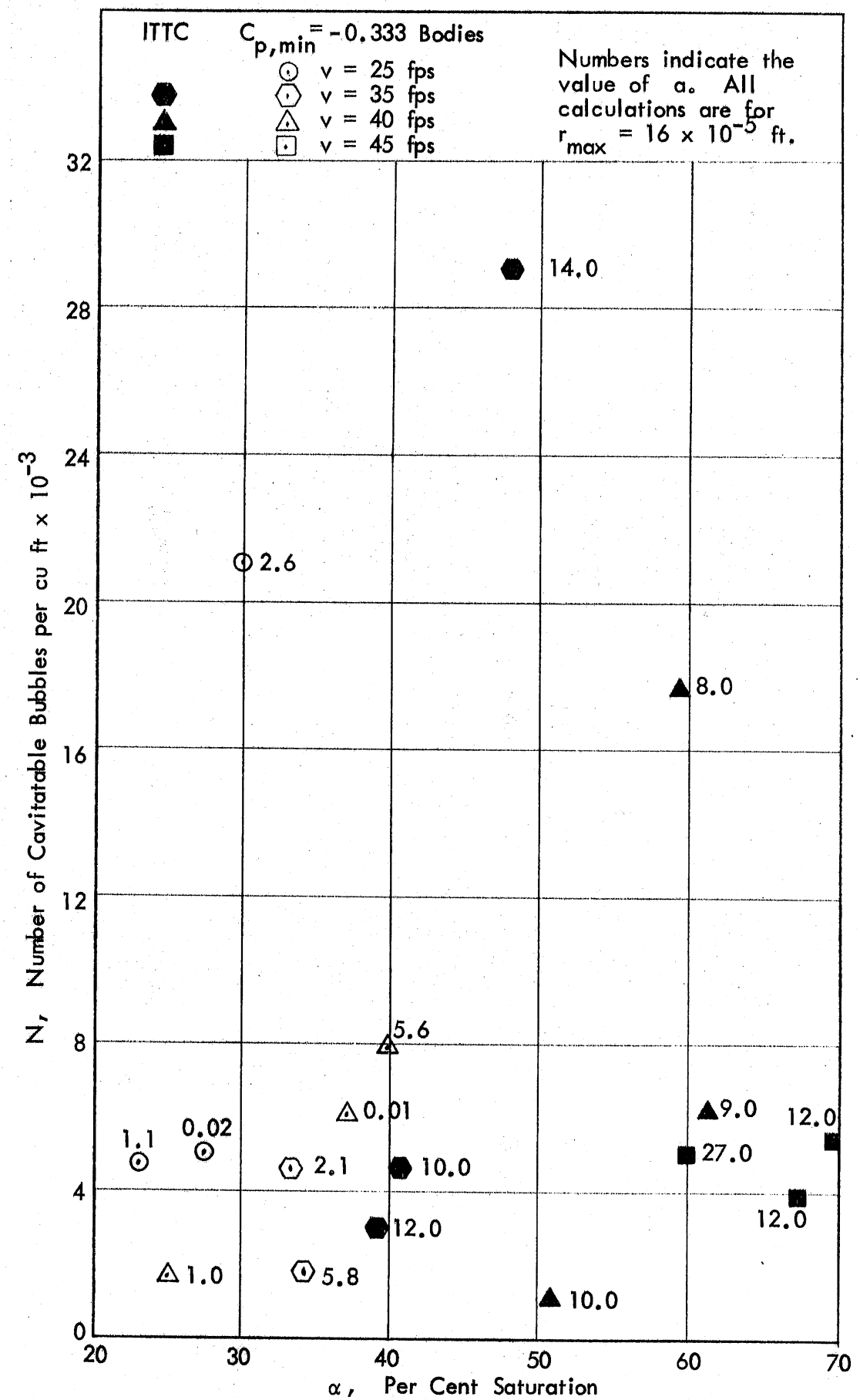

Fig. 7 - Density of Cavitatable Bubbles as a function of Total Air Content

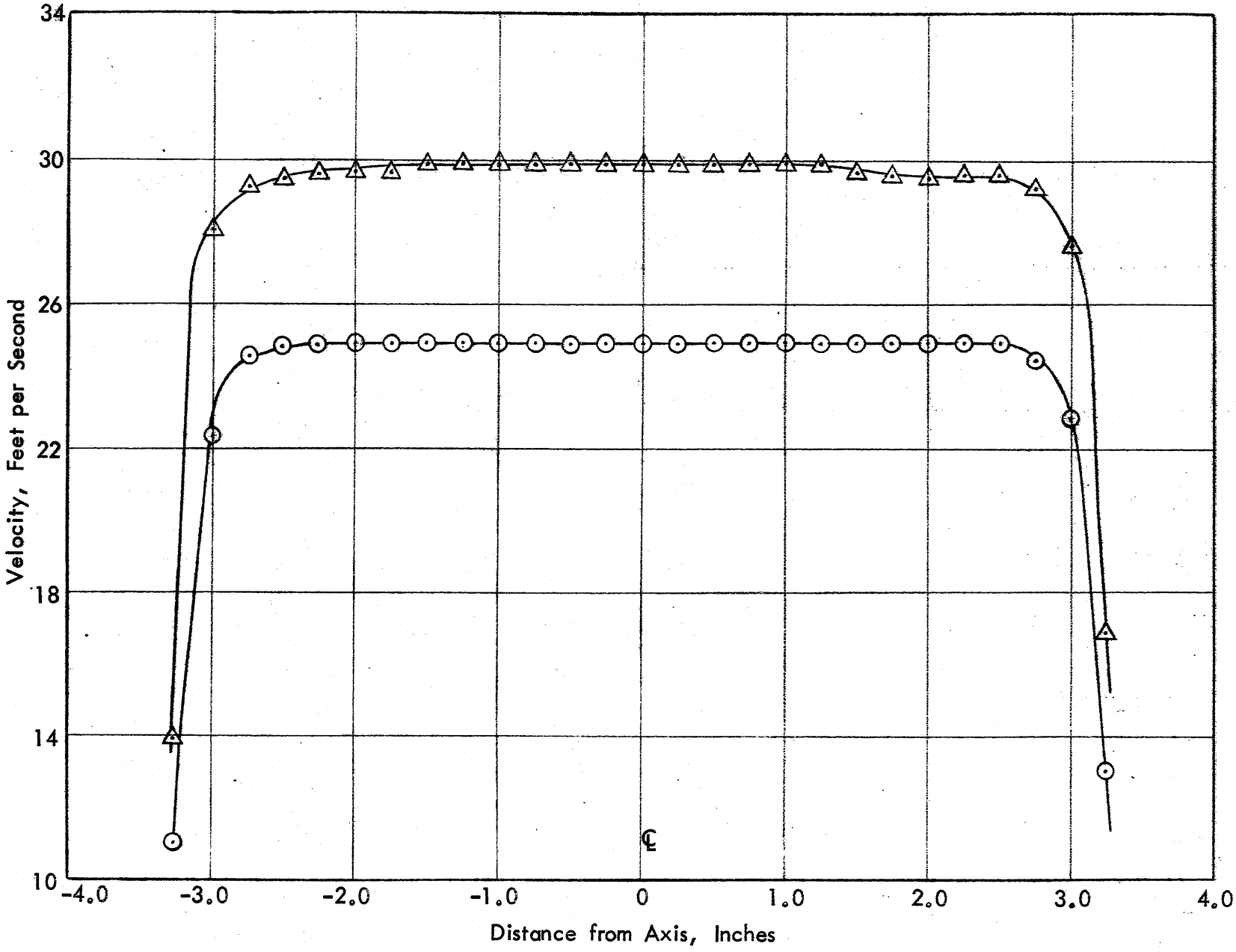

Fig. 8 - Velocity Profiles, Open Jet Test Section, Six-Inch Water Tunnel

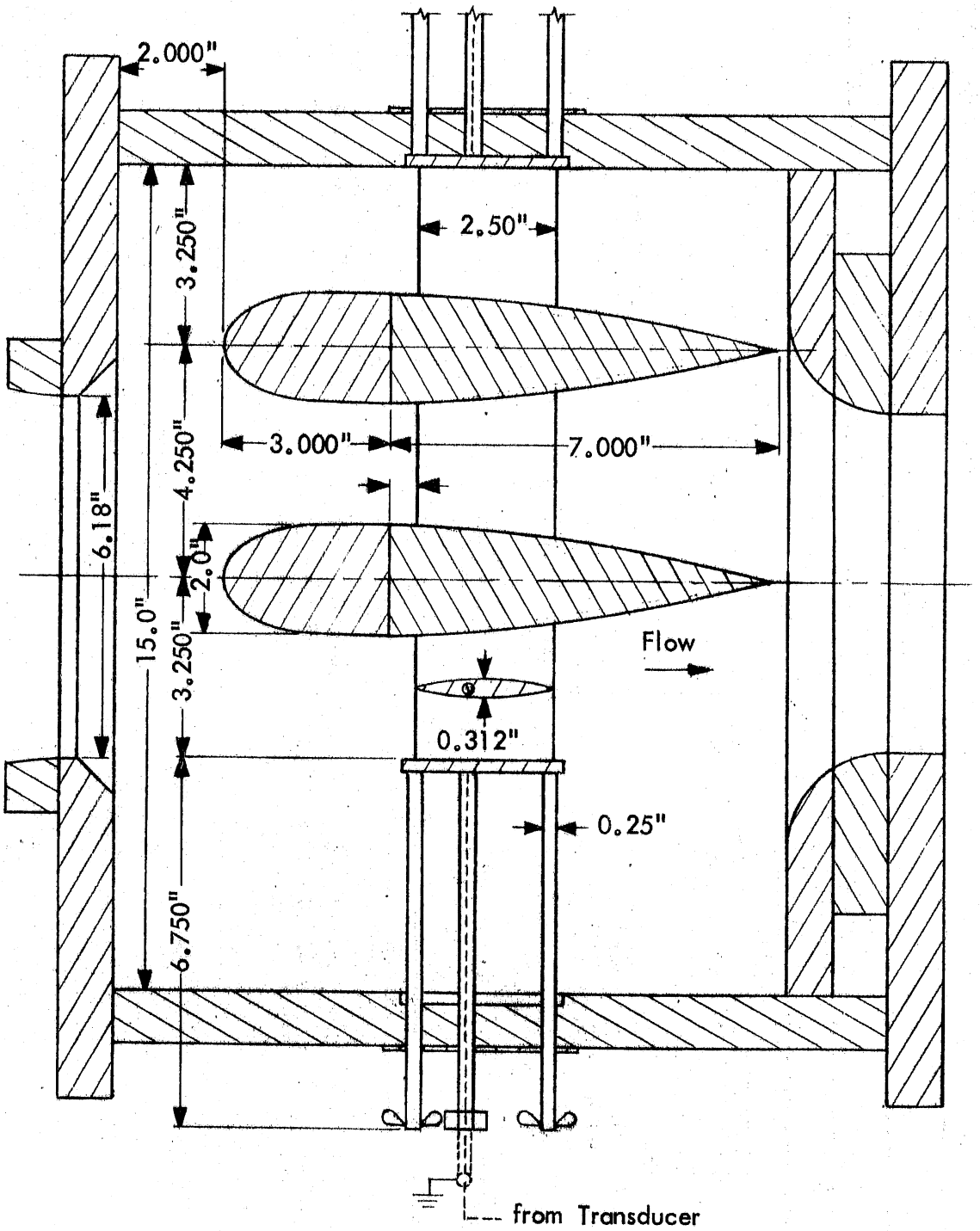

Fig. 9 - Test Bodies in Open Jet Test Section

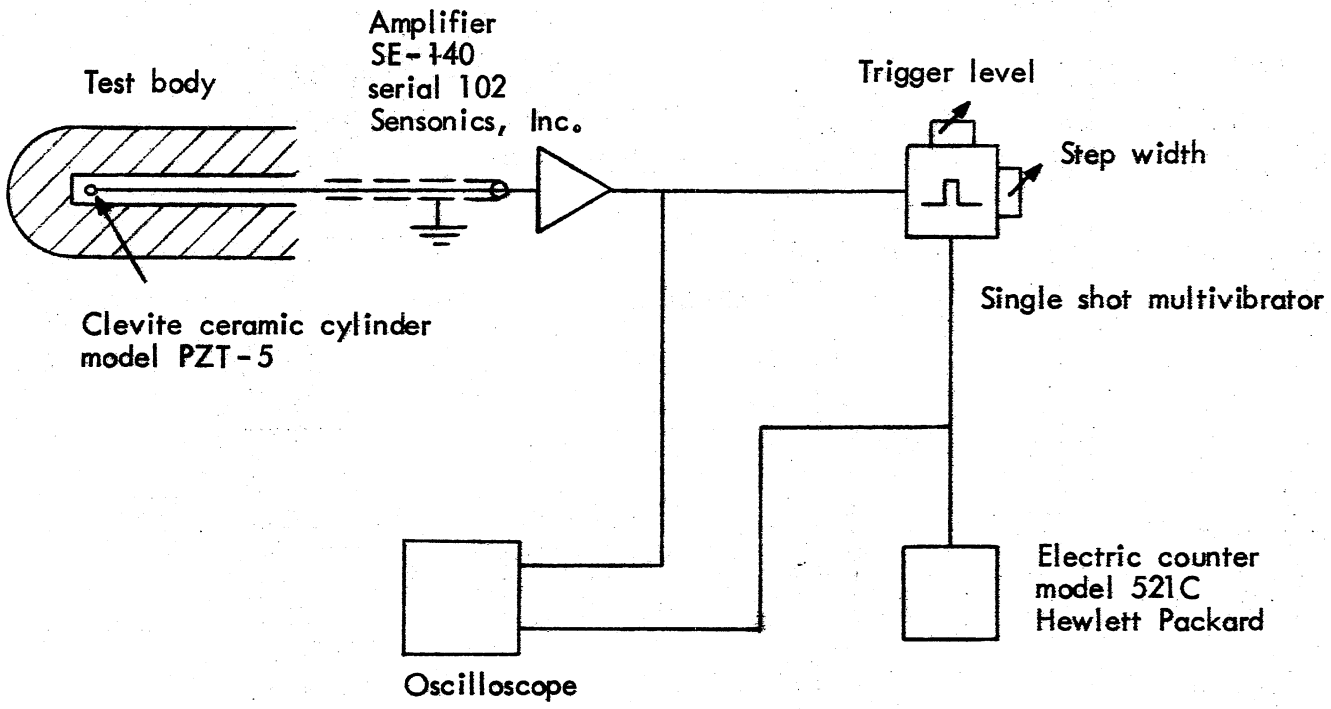

Fig. 10 - Schematic of Transducer Electronics

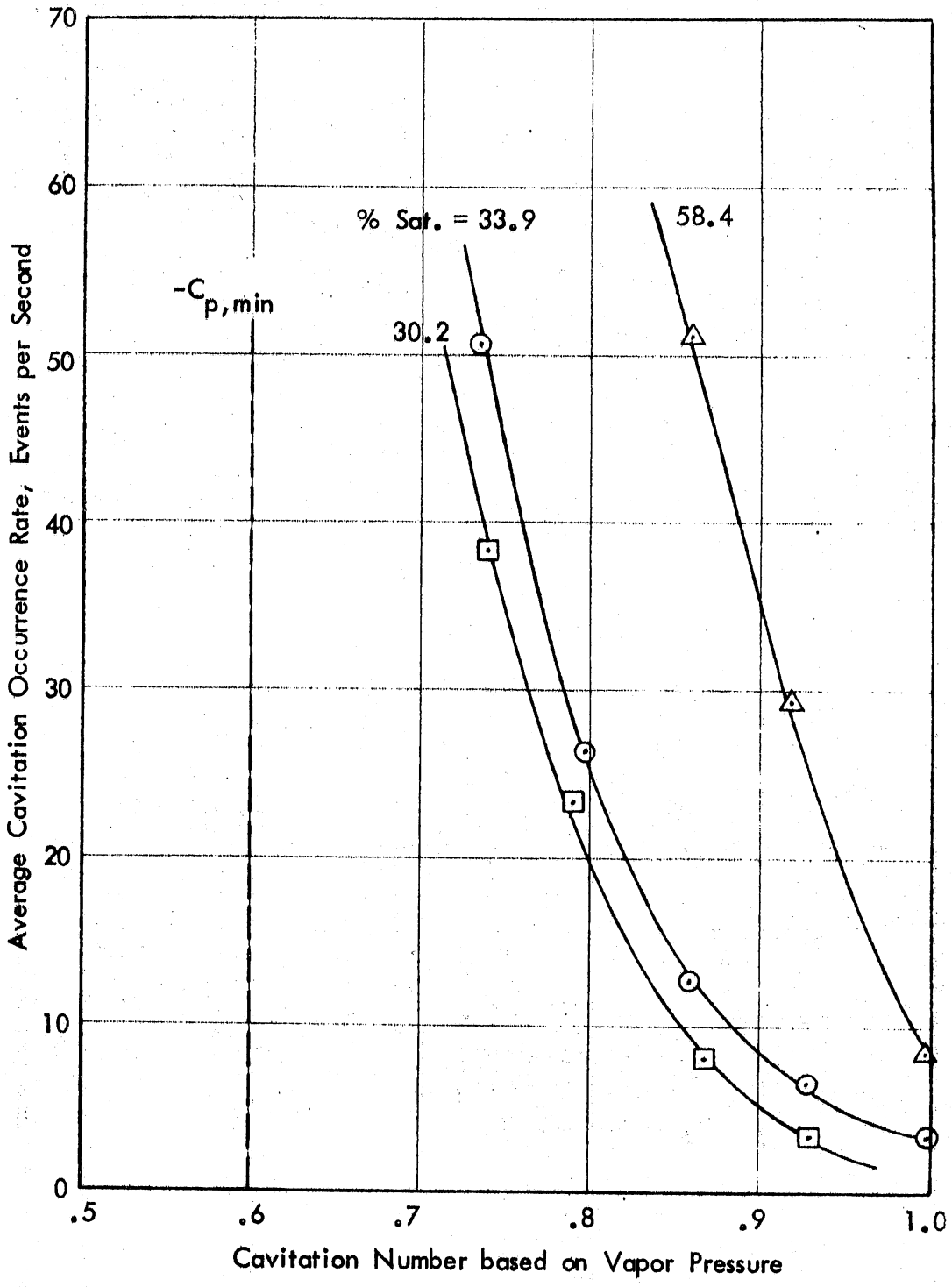

Fig. 11 - Typical Measured Cavitation Characteristics in the Open Jet Test Section, $C_{p,min}$ = -0.60 Body

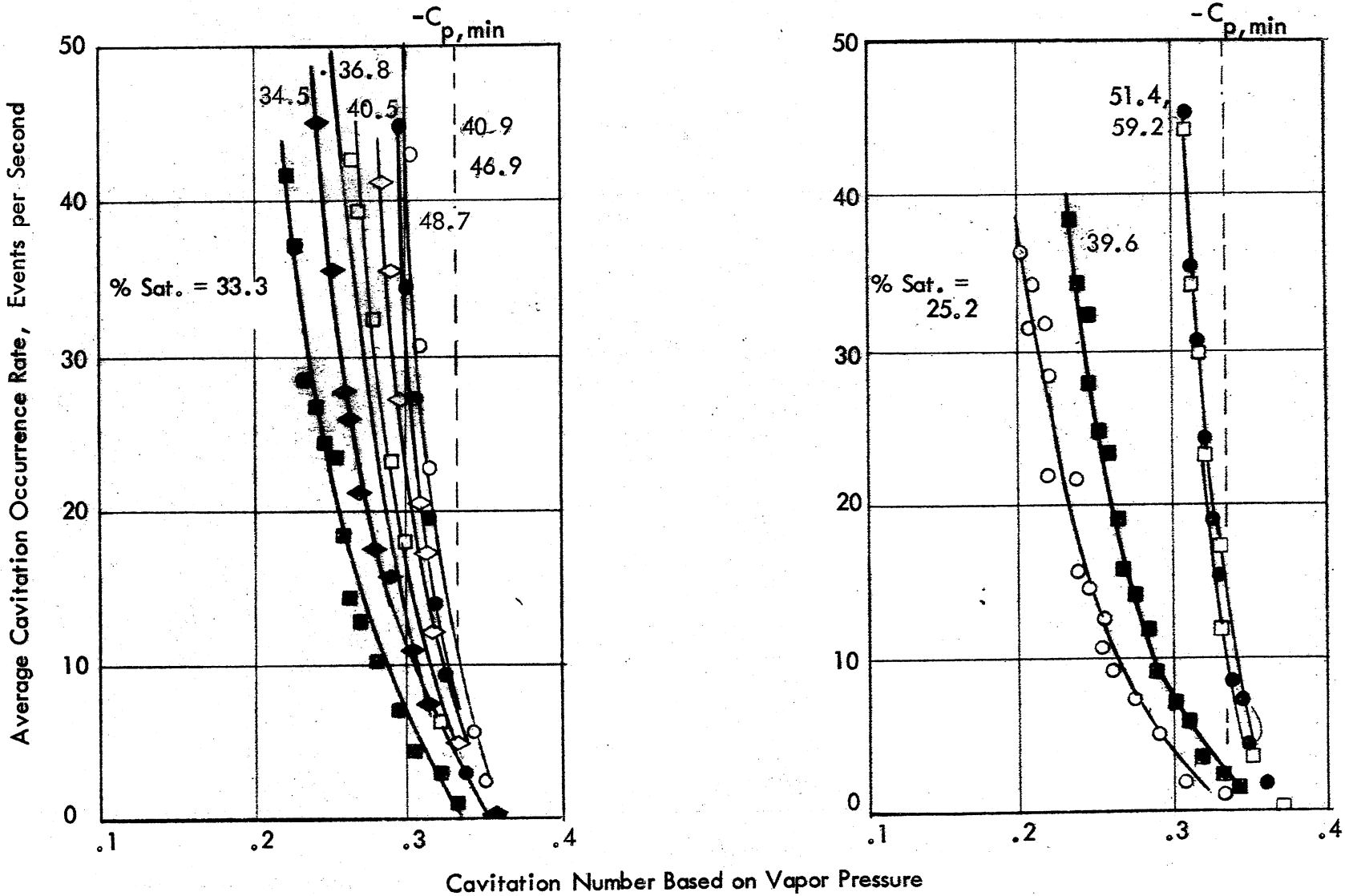

a. 35 ft per sec

b. 40 ft per sec

Fig. 12 - Typical Measured Cavitation Occurrence Characteristics in the Closed Jet Test Section, $C_{p,min}$ = -0.333 Body [23]

APPENDIX I

Cavitation Nuclei

From the viewpoint of amenability to calculation, small spherical gas bubbles would be desirable nuclei. Peterson [6] has shown by holographic photography that such nuclei do exist, but he has also shown that they are intermixed with solid particles. The latter are assumed to be Harvey nuclei [26], hydrophobic particles with fissures containing stabilized gas pockets. In reviewing work by others as related to his own work, Peterson reports that small gas bubbles collect microscopic particles which coagulate as the bubbles shrink to form Harvey nuclei, thus explaining the solid particles he has observed. These particles are assumed to be of nearly neutral density, and this property permits them to subsist in towing tanks and open water for long periods of time.

Turner [27] visualizes the solid-appearing nuclei as being formed by the same microscopic particles as Peterson saw, but with the particles producing a thick, compacted skin perhaps bound by organic compounds. Gas remains on the inside, being prevented from diffusing by the compacted skin. The nucleus so formed is assumed to approach neutral buoyancy. One of the authors [28], referring to the dissolution of bubbles in water under observation through a microscope in a rotating fluid, commented as follows:

> Occasionally a speck of dirt would be trapped on a bubble surface and appeared to be held rigidly in the surface.... Dirt specks definitely reduced the rate of solution and runs where dirt was picked up were discontinued. Once a bubble surface was completely covered with a dirt crust, after it had shrunk to a certain size it failed to shrink further regardless of increase in pressure or speed, being entirely insulated by the crust.

Lieberman [29] made similar observations on a static bubble.

Turner's hypothesis leads to a conceptual model of an ideal nucleus for cavitation purposes. A nucleus is assumed to be a gas bubble encased in an impermeable skin of such density that the nucleus has neutral buoyancy. This makes it possible to take the nuclei as following closely the streamlines of the flow, but otherwise behaving like spherical gas bubbles with respect to cavitation. They simply expand when the pressure is first reduced in accordance with the isothermal gas laws and when they become

larger, the particles are sufficiently dispersed on the surface that vaporous cavitation can occur. This is the model used herein. True gas bubble nuclei have different trajectories, and these can be calculated for a refined model, although the trajectories do not vary too far from the streamlines if the body is large compared to the nuclei. Likewise, true solid nuclei do not behave like spherical gas bubbles at first, and refined models would have to allow for this. But the model does facilitate further computation and is probably sufficiently representative of real nuclei to be useful.

APPENDIX II

Boundary Layer Separation on the Standard Bodies

Calculations for laminar boundary layer separation were made using Stratford's method [19, pp. 324-329] with

$$S = X^2 \, Cp^*\left(\frac{dCp^*}{dx}\right)^2 \Bigg|_{\text{separation}} = 0.0104 \qquad \text{(II-1)}$$

$$Cp^* = \frac{p - p_{min}}{\frac{1}{2} \rho \, U_{max}^{\,2}} \qquad \text{(II-2)}$$

Here X is measured along the body surface from an artificial origin somewhere upstream of the minimum pressure point. The origin is determined by assuming that the boundary layer upstream of the point of minimum pressure is a constant pressure layer and making the momentum thickness of this constant pressure layer the same as that of the real boundary layer. The real boundary layer momentum thickness is estimated from Thwaites's formula as adapted to axisymmetrical bodies [19, p. 432].

A machine program was used to calculate and print S versus X for several bodies from the body coordinates and the previously calculated surface pressures. The results are shown in Table II-1. In the table, X is measured in body radii and

$$Cp = \frac{p - p_o}{\frac{1}{2} \rho \, U_o^{\,2}} \qquad \text{(II-3)}$$

where p_o and U_o are the upstream ambient pressure and velocity.

The calculations show that none of the disk source bodies are subject to laminar separation. The ITTC headform should experience laminar separation if transition to turbulence does not occur first. This is confirmed by Arakeri [18], but the present calculation shows separation a little farther along the body. Data from the 5/8 in. diameter ITTC headform were used in this report. The X-Reynolds number at separation is of the order of 3×10^5 or higher for these data, and it is very likely that separation was prevented by transition.

Table II-1 -- CALCULATED RESULTS FOR STRATFORD'S SEPARATION PARAMETER

a. $c_{pmin} = -0.333$

$-c_p$	x	S
0.333	0.403	0.0000
0.333	0.429	0.0000
0.331	0.481	0.0000
0.327	0.532	0.0000
0.320	0.583	0.0001
0.3125	0.710	0.0003
0.274	0.912	0.0011
0.233	1.113	0.0021
0.196	1.314	0.0027
0.165	1.514	0.0029
0.139	1.714	0.0028
0.118	1.914	0.0022
		*

$S < 0.0104$
No Separation

b. $c_{pmin} = -0.45$

$-c_p$	x	S
0.450	0.231	0.0000
0.450	0.242	0.0000
0.447	0.285	0.0000
0.444	0.328	0.0000
0.430	0.370	0.0001
0.424	0.391	0.0001
0.418	0.411	0.0002
0.412	0.473	0.0004
0.379	0.576	0.0010
0.346	0.677	0.0018
0.314	0.778	0.0024
0.285	0.880	0.0031
0.259	0.981	0.0036
0.235	1.081	0.0039
0.214	1.331	0.00415
0.148	1.732	0.0035
0.1065	2.132	0.0025
		*

$S < 0.0104$
No Separation

*Continuous decrease thereafter

Table II-1 [Continued]

c. $c_{pmin} = -0.600$

$-c_p$	x	S
0.600	0.137	0.0000
0.600	0.148	0.0000
0.594	0.171	0.0000
0.585	0.194	0.0000
0.574	0.216	0.0001
0.562	0.238	0.0002
0.549	0.259	0.0003
0.536	0.281	0.0005
0.524	0.302	0.0006
0.511	0.323	0.0008
0.499	0.344	0.0010
0.487	0.365	0.0012
0.475	0.386	0.0014
0.464	0.407	0.0016
0.453	0.469	0.0022
0.403	0.571	0.0032
0.359	0.672	0.0040
0.321	0.773	0.0045
0.289	0.874	0.0049
0.260	0.975	0.0051
0.235	1.075	0.0052
0.213	1.325	0.0049
0.147	1.726	0.0037
		*

d. $c_{pmin} = -0.800$

$-c_p$	x	S
0.800	0.073	0.0000
0.800	0.086	0.0000
0.782	0.111	0.0001
0.751	0.135	0.0004
0.719	0.159	0.0007
0.689	0.180	0.0011
0.661	0.203	0.0014
0.636	0.225	0.0018
0.612	0.246	0.0021
0.590	0.268	0.0024
0.570	0.289	0.0027
0.552	0.310	0.0029
0.534	0.331	0.0032
0.518	0.352	0.0034
0.502	0.373	0.0036
0.488	0.393	0.0038
0.474	0.455	0.0043
0.414	0.557	0.0050
0.365	0.659	0.0055
0.324	0.760	0.0057
0.290	0.860	0.0058
0.260	0.961	0.0057
0.235	1.061	0.0056
		*

e. $c_{pmin} = -1.00$

$-c_p$	x	S
1.000	0.047	0.0000
1.000	0.053	0.0000
0.989	0.072	0.0002
0.920	0.097	0.0010
0.852	0.121	0.0018
0.796	0.144	0.0025
0.749	0.167	0.0030
0.709	0.189	0.0034
0.675	0.211	0.0037
0.645	0.233	0.0039
0.618	0.254	0.0041
0.594	0.275	0.0043
0.572	0.296	0.0045
0.551	0.317	0.0046
0.532	0.338	0.0048
0.515	0.359	0.0049
0.499	0.380	0.0050
0.419	0.441	0.0053
0.368	0.544	0.0057
0.326	0.645	0.0058
0.290	0.746	0.0059
0.260	0.847	0.0058
0.234	0.947	0.0056
0.212	0.047	0.0054
		*

f. ITTC Headform

$-c_p$	x	S
0.580	0.366	0.0000
0.579	0.395	0.0000
0.577	0.454	0.0000
0.571	0.512	0.0000
0.560	0.570	0.0002
0.544	0.628	0.0006
0.524	0.685	0.0018
0.497	0.742	0.0053
---SEPAR.------		
0.462	0.799	0.0176
0.412	0.856	0.0540
0.344	0.916	0.0584
		*

*Continuous decrease thereafter

APPENDIX III

Fitting Calculated Cavitation Characteristics to Measured Characteristics

For a given standard body and using the exponential nucleus size distribution given by Eq. (4), Eq. (3) states in effect that the calculated cavitation rate is

$$M_c = M(\sigma, N, r_{max}, a) \qquad \text{(III-1)}$$

On the other hand, measured occurrence rates for the same body are determined by

$$M_m = M(\sigma, \alpha, \text{other factors}) \qquad \text{(III-2)}$$

where α is the relative total gas content of the experimental water and the "other factors" include the real nuclei characteristics (including the number of cavitatable nuclei) and their relation to α and the tunnel operating conditions. However, only σ and α are specifically measurable.

Matching a calculated curve to a measured one is largely a matter of trial and error. The process can be simplified by working with M ratios at pairs of M versus σ points obtained experimentally for fixed α. In the calculations this eliminates N as a parameter. From Eq. (3)

$$\frac{M_1}{M_2} = \frac{\Sigma[c_{ij}]_1[m_i]}{\Sigma[c_{ij}]_2[m_i]} \qquad \text{(III-3)}$$

and m_i is sought where M_1/M_2 is measured. The trial-and-error process consists of carrying out the indicated operations.

The matrix c_{ij} can be readily determined from [2] for each body at each σ for a given r_{max}. A number of m_i matrices are then computed from Eq. (4) for a range of a. If $0.0 \leqslant a \leqslant 30.0$ and an increment of 0.01 in a is chosen, 3000 column matrices are calculated. These m_i matrices are stored on magnetic tape and are available for all future calculations as long as $i_{max} = 16$. The solution to Eq. (III-3) is found by comparing the measured ratio M_1/M_2 with the computed ratio for the various m_i matrices.

Because of the random nature of cavitation data, a range of a values will solve Eq. (III-3) within certain error limits. It is useful, therefore, to solve Eq. (III-3) for two or three pairs of measured ratios to obtain an average value of a which is valid along the entire characteristic curve (within the test σ range). Data points selected for the computations in this paper are indicated in Figs. 1 and 2.

Once a has been determined, N can be found from Eq. (3) as follows:

$$N = \frac{M_{(\sigma)}}{q\Sigma\left[c_{ij}(\sigma, r_{max})\right] m_i(a)} \qquad \text{(III-4)}$$

for one of the measured points.

DISTRIBUTION LIST FOR PROJECT REPORT NO. 141

of the St. Anthony Falls Hydraulic Laboratory

Copies	Organization
12	Defense Documentation Center, Cameron Station, Alexandria, Virginia 22314
1	Technical Library, Naval Ship Research and Development Laboratory, Annapolis, Maryland 21402
1	Professor Bruce Johnson, Engineering Department, Naval Academy, Annapolis, Maryland 21402
1	Library, Naval Academy, Annapolis, Maryland 21402
1	Professor W. P. Graebel, Department of Engineering Mechanics, College of Engineering, University of Michigan, Ann Arbor, Michigan 48108
1	Professor T. Francis Ogilvie, Department of Naval Architecture and Marine Engineering, University of Michigan, Ann Arbor, Michigan 48108
1	AFOSR (REM), 1400 Wilson Boulevard, Arlington, Virginia 22204
1	Professor S. Corrsin, Department of Mechanics and Materials Science, The Johns Hopkins University, Baltimore, Maryland 21218
1	Professor R. B. Couch, Department of Naval Architecture and Marine Engineering, The University of Michigan, Ann Arbor, Michigan 48105
1	Professor O. M. Phillips, Department of Mechanics and Materials Science, The Johns Hopkins University, Baltimore, Maryland 21218
1	Librarian, Department of Naval Architecture, University of California, Berkeley, California 94720
1	Professor J. R. Paulling, Institute of Engineering Research, Department of Naval Architecture, University of California, Berkeley, California 94720
1	Professor W. C. Webster, College of Engineering, Department of Naval Architecture, University of California, Berkeley, California 94720
1	Professor J. V. Wehausen, Institute of Engineering Research, Department of Naval Architecture, University of California, Berkeley, California 94720
1	Commander, Boston Naval Shipyard, Boston, Massachusetts 02129
1	Director, Office of Naval Research Branch Office, 495 Summer Street, Boston, Massachusetts 02210
1	Commander, Puget Sound Naval Shipyard, Bremerton, Washington 98314

Copies	Organization
1	Professor G. Birkhoff, Department of Mathematics, Harvard University, Cambridge, Massachusetts 02139
1	Professor G. F. Carrier, Division of Engineering and Applied Physics, Harvard University, Cambridge, Massachusetts 02139
1	Commanding Office, NROTC Naval Administrative Unit, Massachusetts Institute of Technology, Cambridge, Massachusetts 02139
1	Professor M. A. Abkowitz, Department of Ocean Engineering, Massachusetts Institute of Technology, Cambridge, Massachusetts 02139
1	Professor A. T. Ippen, Department of Civil Engineering, Massachusetts Institute of Technology, Cambridge, Massachusetts 02139
1	Professor Phillip Mandel, Department of Ocean Engineering, Massachusetts Institute of Technology, Cambridge, Massachusetts 02139
1	Professor E. Mollo-Christensen, Department of Meteorology, Room 54-1722, Massachusetts Institute of Technology, Cambridge, Massachusetts 02139
1	Professor J. Nicholas Newman, Department of Ocean Engineering, Room 5-324A, Massachusetts Institute of Technology, Cambridge, Massachusetts 02139
1	Commander, Charleston Naval Shipyard, Naval Base, Charleston, South Carolina 29408
1	A. R. Kuhlthau, Director, Research Laboratories for the Engineering Sciences, Thornton Hall, University of Virginia, Charlottesville, Virginia 22903
1	Director, Office of Naval Research Branch Office, 536 South Clark Street, Chicago, Illinois 60605
1	Library, Naval Weapons Center, China Lake, California 93555
1	Professor J. M. Burgers, Institute of Fluid Dynamics and Applied Mathematics, University of Maryland, College Park, Maryland 20742
1	Professor Pai, Institute for Fluid Dynamics and Applied Mathematics, University of Maryland, College Park, Maryland 20740
1	Acquisition Director, NASA Scientific and Technical Information, P.O. Box 33, College Park, Maryland 20740
1	Technical Library, Naval Weapons Laboratory, Dahlgren, Virginia 22448
1	Dr. C. S. Wells, Jr., Advanced Technology Center, Inc., P.O. Box 6144, Dallas, Texas 75222
1	Commanding Officer, Army Research Office, Box CM, Duke Station, Durham, North Carolina 27706

Copies	Organization
1	Technical Documents Center, Building 315, U.S. Army Mobility Equipment Research and Development Center, Fort Belvoir, Virginia 22060
1	Professor J. E. Cermak, Department of Atmospheric Sciences, Colorado State University, Fort Collins, Colorado 80521
1	Technical Library, Webb Institute of Naval Architecture, Glen Cove, Long Island, New York 11542
1	Professor E. V. Lewis, Webb Institute of Naval Architecture, Glen Cove, Long Island, New York 11542
1	Dr. M. Poreh, Technion-Israel Institute of Technology, Department of Civil Engineering, Haifa, Israel
1	Dr. B. N. Pridmore Brown, Northrop Corporation, NORAIR-Division, Hawthorne, California 90250
1	Dr. J. P. Breslin, Davidson Laboratory, Stevens Institute of Technology, Castle Point Station, Hoboken, New Jersey 07030
1	Mr. C. H. Henry, Stevens Institute of Technology, Davidson Laboratory, Castle Point Station, Hoboken, New Jersey 07030
1	Dr. D. Savitsky, Davidson Laboratory, Stevens Institute of Technology, Castle Point Station, Hoboken, New Jersey 07030
1	Dr. A. Strumpf, Davidson Laboratory, Stevens Institute of Technology, Castle Point Station, Hoboken, New Jersey 07030
1	Dr. J. P. Craven, University of Hawaii, 1801 University Avenue, Honolulu, Hawaii 96822
1	Professor J. F. Kennedy, Director, Iowa Institute of Hydraulic Research, State University of Iowa, Iowa City, Iowa 52240
1	Professor L. Landweber, Iowa Institute of Hydraulic Research, State University of Iowa, Iowa City, Iowa 52240
1	Director, Scripps Institute of Oceanography, University of California, La Jolla, California 92037
1	Professor A. T. Ellis, University of California, San Diego, Department of Aerospace and Mechanical Engineering Science, La Jolla, California 92037
1	Dr. Coda Pan, Mechanical Technology Incorporated, 968 Albany-Shaker Road, Latham, New York 12110
1	Mr. P. Eisenberg, President, Hydronautics, Incorporated, 8210 Pindell School Road, Laurel, Maryland 20810

Copies	Organization
1	Mr. M. P. Tulin, Hydronautics, Incorporated, 8210 Pindell School Road, Laurel, Maryland 20810
1	Commander, Long Beach Naval Shipyard, Long Beach, California 90802
1	Dr. John M. Killen, St. Anthony Falls Hydraulic Laboratory, University of Minnesota, Minneapolis, Minnesota 55455
1	Lorenz G. Straub Library, St. Anthony Falls Hydraulic Laboratory, University of Minnesota, Minneapolis, Minnesota 55455
1	Professor J. Ripken, St. Anthony Falls Hydraulic Laboratory, University of Minnesota, Minneapolis, Minnesota 55455
1	Professor E. Silberman, Director, St. Anthony Falls Hydraulic Laboratory, University of Minnesota, Minneapolis, Minnesota 55455
1	Superintendent, Naval Postgraduate School, Attn: Library, Monterey, California 93940
1	Professor A. B. Metzner, Department of Chemical Engineering, University of Delaware, Newark, New Jersey 19711
1	Technical Library, Naval Underwater Systems Center, Newport, Rhode Island 02840
1	Office of Naval Research, New York Area Office, 207 W. 24th Street, New York, New York 10011
1	Professor V. Castelli, Department of Mechanical Engineering, Columbia University, New York, New York 10027
1	Professor H. Elrod, Department of Mechanical Engineering, Columbia University, New York, New York 10017
1	Engineering Societies Library, 345 East 47th Street, New York, New York 10017
1	Society of Naval Architects and Marine Engineers, 74 Trinity Place, New York, New York 10006
1	Miss O. M. Leach, Librarian, National Research Council, Aeronautical Library, Montreal Road, Ottawa 7, Canada
1	Technical Library, Naval Coastal System Laboratory, Panama City, Florida 32401
1	Dr. J. W. Hoyt, Naval Undersea R and D Center, Pasadena Laboratory, 3202 E. Foothill Boulevard, Pasadena, California 91107
1	Technical Library, Naval Undersea R and D Center, Pasadena Laboratory, 3203 E. Foothill Boulevard, Pasadena, California 91107

Copies	Organization
1	Professor A. J. Acosta, Department of Mechanical Engineering, California Institute of Technology, Pasadena, California 91109
1	Professor H. Liepmann, Graduate Aeronautical Laboratory, California Institute of Technology, Pasadena, California 91109
1	Professor M. S. Plesset, Department of Engineering Science, California Institute of Technology, Pasadena, California 91109
1	Professor T. Y. Wu, Department of Engineering Science, California Institute of Technology, Pasadena, California 91109
1	Director, Office of Naval Research Branch Office, 1030 E. Green Street, Pasadena, California 91106
1	Naval Ship Engineering Center, Philadelphia Division, Technical Library, Philadelphia, Pennsylvania 19112
1	Technical Library, Philadelphia Naval Shipyard, Philadelphia, Pennsylvania 19112
1	Dr. Paul Kaplan, Oceanics, Inc., Technical Industrial Park, Plainview, New York 11803
1	Technical Library, Naval Missile Center, Point Mugu, California 93441
1	Technical Library, Naval Civil Engineering Laboratory, Port Hueneme, California 93041
1	Commander, Portsmouth Naval Shipyard, Portsmouth, New Hampshire 03801
1	Commander, Norfolk Naval Shipyard, Portsmouth, Virginia 23709
1	Dr. H. N. Abramson, Southwest Research Institute, 8500 Culebra Road, San Antonio, Texas 78206
1	Editor, Applied Mechanics Review, Southwest Research Institute, 8500 Culebra Road, San Antonio, Texas 78206
1	Dr. Andrew Fabula, Code 600, Building 106, Naval Undersea R and D Center, San Diego, California 92132
1	Office of Naval Research, San Francisco Area Office, 760 Market Street, Room 447, San Francisco, California 94102
1	Library, Pearl Harbor Naval Shipyard, Box 400, FPO, San Francisco, California 96610
1	Technical Library, Hunters Point Naval Shipyard, San Francisco, California 94135
1	Librarian, Naval Ordnance Laboratory, White Oak, Silver Spring, Maryland 20910

Copies	Organization
1	Fenton Kennedy Document Library, The Johns Hopkins University, Applied Physics Laboratory, 8621 Georgia Avenue, Silver Spring, Maryland 20910
1	Professor R. C. DiPrima, Department of Mathematics, Rensselaer Polytechnic Institute, Troy, New York 12181
1	Professor J. W. Holl, The Pennsylvania State University, Institute for Science and Engineering, Applied Research Laboratory, P.O. Box 30, State College, Pennsylvania 16801
1	Professor J. Lumley, The Pennsylvania State University, Institute for Science and Engineering, Applied Research Laboratory, P.O. Box 30, State College, Pennsylvania 16801
1	Dr. J. M. Robertson, Department of Theoretical and Applied Mechanics, University of Illinois, Urbana, Illinois 61801
1	Technical Library, Mare Island Naval Shipyard, Vallejo, California 94592
3	Code 438, Office of Naval Research, Department of the Navy, Arlington, Virginia 22217
1	Code 463, Office of Naval Research, Department of the Navy, Arlington, Virginia 22217
1	Code 466, Office of Naval Research, Department of the Navy, Arlington, Virginia 22217
1	Code 468, Office of Naval Research, Department of the Navy, Arlington, Virginia 22217
1	Code 473, Office of Naval Research, Department of the Navy, Arlington, Virginia 22217
1	Code 481, Office of Naval Research, Department of the Navy, Arlington, Virginia 22217
6	Code 2627, Naval Research Laboratory, Washington D.C. 20375
6	Library, Code 2629 (ONRL), Naval Research Laboratory, Washington, D.C. 20375
1	Code 6170, Naval Research Laboratory, Washington, D.C. 20375
1	Code 4000, Director of Research, Naval Research Laboratory, Washington, D.C. 20375
1	Code 8030 (Maury Center), Naval Research Laboratory, Washington, D.C. 20375
1	Code 8040, Naval Research Laboratory, Washington, D.C. 20375

Copies	Organization
1	Code 031, Naval Ship Systems Command, Washington, D.C. 20362
1	Code 0341, Naval Ship Systems Command, Washington, D.C. 20362
1	Code 03Z2 (L. Benen), Naval Ship Systems Command, Washington, D.C. 20362
1	Code 03Z1 (J. Schuler), Naval Ship Systems Command, Washington, D.C. 20362
1	Code 2052, Naval Ship Systems Command, Washington, D.C. 20362
1	Code 6034, Naval Ship Engineering Center, Center Building, Prince George's Center, Hyattsville, Maryland 20782
1	Code 6101E, Naval Ship Engineering Center, Center Building, Prince George's Center, Hyattsville, Maryland 20782
1	Code 6110, Naval Ship Engineering Center, Center Building, Prince George's Center, Hyattsville, Maryland 20782
1	Code 6114, Naval Ship Engineering Center, Center Building, Prince George's Center, Hyattsville, Maryland 20782
1	Code 6120E, Naval Ship Engineering Center, Center Building, Prince George's Center, Hyattsville, Maryland 20782
1	Code 6136, Naval Ship Engineering Center, Center Building, Prince George's Center, Hyattsville, Maryland 20782
1	Dr. A. Powell (Code 01), Naval Ship Research and Development Center, Bethesda, Maryland 20034
1	Mr. W. M. Ellsworth (Code 11), Naval Ship Research and Development Center, Bethesda, Maryland 20034
1	Dr. W. E. Cummins (Code 15), Naval Ship Research and Development Center, Bethesda, Maryland 20034
1	Mr. R. Wermter (Code 152), Naval Ship Research and Development Center, Bethesda, Maryland 20034
1	Dr. W. B. Morgan (Code 154), Naval Ship Research and Development Center, Bethesda, Maryland 20034
1	Mr. J. B. Hadler (Code 156), Naval Ship Research and Development Center, Bethesda, Maryland 20034
1	Library (Code 5641), Naval Ship Research and Development Center, Bethesda, Maryland 20034
1	Mr. S. F. Crump (Code 1505), Naval Ship Research and Development Center, Bethesda, Maryland 20034

Copies	Organization
1	Dr. P. Pien (Code 1521), Naval Ship Research and Development Center, Bethesda, Maryland 20034
1	Mr. Paul Granville (Code 1541), Naval Ship Research and Development Center, Bethesda, Maryland 20034
1	Mr. J. McCarthy (Code 1552), Naval Ship Research and Development Center, Bethesda, Maryland 20034
1	Dr. Nils Salvesen (Code 1552), Naval Ship Research and Development Center, Bethesda, Maryland 20034
1	Dr. M. Strasberg (Code 1901), Naval Ship Research and Development Center, Bethesda, Maryland 20034
1	Code 03, Naval Air Systems Command, Department of the Navy, Washington, D.C. 20361
1	AIR 5301, Naval Air Systems Command, Department of the Navy, Washington, D.C. 20361
1	AIR 604, Naval Air Systems Command, Department of the Navy, Washington, D.C. 20361
1	Code ORD 03, Naval Ordnance Systems Command, Department of the Navy, Washington, D.C. 20360
1	Code ORD 035, Naval Ordnance Systems Command, Department of the Navy, Washington, D.C. 20360
1	Code ORD 05413, Naval Ordnance Systems Command, Department of the Navy, Washington, D.C. 20360
1	Code ORD 9132, Naval Ordnance Systems Command, Department of the Navy, Washington, D.C. 20360
1	CNM PM-1, Strategic Systems Project Office, Department of the Navy, Washington, D.C. 20360
1	Technical Division (CNM PM 11-20), Deep Submergence Systems Project Office, Department of the Navy, Washington, D.C. 20360
1	Oceanographer of the Navy, Washington, D.C. 20373
1	Commander, Naval Oceanographic Office, Washington, D.C. 20373
1	Dr. A. L. Slafkosky, Scientific Adviser, Commandant of the Marine Corps (Code AX), Washington, D.C. 20380
1	Librarian Station 5-2, Coast Guard Headquarters, NASSIF Building, 400 - 7th Street, S. W., Washington, D.C. 20591

Copies	Organization
1	Office of Research and Development, Maritime Administration, 441 G Street, N. W., Washington, D.C. 20035
1	Division of Ship Design, Maritime Administration, 441 G Street, N. W., Washington, D.C. 20235
1	National Science Foundation, Engineering Division, 1800 G Street, N. W., Washington, D.C. 20550
1	Dr. G. Kulin, National Bureau of Standards, Washington, D.C. 20234
1	Science and Technology Division, Library of Congress, Washington, D.C. 20540
1	Chief of Research and Development, Office of Chief of Staff, Department of the Army, Washington, D.C. 20310
1	Professor A. Thiruvengadam, Department of Mechanical Engineering, The Catholic University of America, Washington, D.C. 20017
1	Professor Bruce H. Adee, Department of Mechanical Engineering, University of Washington, Seattle, Washington 98105
1	Mr. Norman Nilsen, General Education Department, California Maritime Academy, P.O. Box 1392, Vallejo, California 94590

Unclassified
Security Classification

DOCUMENT CONTROL DATA - R & D

(Security classification of title, body of abstract and indexing annotation must be entered when the overall report is classified)

1. ORIGINATING ACTIVITY *(Corporate author)*

St. Anthony Falls Hydraulic Laboratory
University of Minnesota

2a. REPORT SECURITY CLASSIFICATION

Unclassified

2b. GROUP

3. REPORT TITLE

THE USE OF STANDARD BODIES TO MEASURE THE CAVITATION STRENGTH OF WATER

4. DESCRIPTIVE NOTES *(Type of report and, inclusive dates)*

Project Report - August 1972 through September 1973

5. AUTHOR(S) *(First name, middle initial, last name)*

Edward Silberman
Frank R. Schiebe
Edward Mrosla

6. REPORT DATE	7a. TOTAL NO. OF PAGES	7b. NO. OF REFS
September 1973	49	29

8a. CONTRACT OR GRANT NO.	9a. ORIGINATOR'S REPORT NUMBER(S)
N00014-67-A-0113-0032	Project Report No. 141
b. PROJECT NO.	
c.	9b. OTHER REPORT NO(S) *(Any other numbers that may be assigned this report)*
d.	

10. DISTRIBUTION STATEMENT

Approved for public release; distribution unlimited

11. SUPPLEMENTARY NOTES	12. SPONSORING MILITARY ACTIVITY
	Office of Naval Research Arlington, Virginia 22217

13. ABSTRACT

Research was conducted to evaluate a technique for measuring the cavitation strength of water. The technique is based on counting cavitation events as a function of cavitation number on a standard body, thereby producing cavitation characteristic curves. It is assumed that water cavitates because of nuclei carried in the water and that the measured characteristic curves must therefore be related to the nuclei which are present.

In this research it was hypothesized that the nuclei, whatever their real nature, could be represented by a distribution of equivalent gas bubbles of neutral density. The standard bodies were designed according to potential flow theory so that the bubble trajectories, along with their cavitation rates, could be calculated. By calculating cavitation characteristic curves for various bubble densities and size distributions and comparing the calculated curves with measured curves for the same body, it was possible to infer the specifications for the equivalent bubble nuclei that were present in any test. The method was partially verified using some available experimental data, but a critical test is yet to be accomplished.

An alternative for future study has been proposed which calls for abandoning the hypothesis of equivalent bubble nuclei and determining the relative cavitation strength of water by direct comparison of a measured cavitation characteristic curve obtained on a standard body in a specific test configuration with a catalogue of such curves kept on file for a family of standard bodies.

DD FORM 1 NOV 65 1473 (PAGE 1)
S/N 0101-807-6811

Unclassified
Security Classification

14 KEY WORDS	LINK A		LINK B		LINK C	
	ROLE	WT	ROLE	WT	ROLE	WT
Cavitation						
Cavitation Inception						
Cavitation Nuclei						